ZIRAT-7 SPECIAL TOPICS REPORT

Corrosion of Zirconium Alloys

Prepared by

Ron Adamson,
Zircology Plus, Fremont, Pleasanton, CA, USA

Brian Cox

Friedrich Garzarolli

Alfred Strasser,
Aquarius Services Corp., Sleepy Hollow, NY, USA

Peter Rudling and Gunnar Wikmark,
Advanced Nuclear Technology Sweden AB, Sweden

December, 2002

Advanced Nuclear Technology International
Uppsala Science Park
SE-751 83 UPPSALA
Sweden

info@antinternational.com

ADVANCED NUCLEAR
TECHNOLOGY INTERNATIONAL

DISCLAIMER

The information presented in this report has been compiled and analysed by Advanced Nuclear Technology International Europe AB (ANT International) and its subcontractors. ANT International has exercised due diligence in this work, but does not warrant the accuracy or completeness of the information. ANT International does not assume any responsibility for any consequences as a result of the use of the information for any party, except a warranty for reasonable technical skill, which is limited to the amount paid for this assignment by each ZIRAT program member.

FOREWORD

This report covers all aspects of Zirconium alloy corrosion. The authors having prepared the different parts of the report all have a vast experience in the field of Zirconium alloy corrosion. However, the authors have different backgrounds and in some cases have different opinions about the Zirconium alloy corrosion mechanisms. The intent of the report is not to dilute the different opinions of the authors (by editing) to such an extent that the reader may believe that there is a consensus. Instead the objective of this report is to allow the different opinions of the authors to stand out, to reflect the fact that there is sometimes different opinions.

Peter Rudling, Editor

CONTENTS

1 INTRODUCTION (F. GARZAROLLI)

In water cooled power reactors, like boiling water reactors (BWRs), pressurized water reactors (PWRs), and pressurized heavy reactors (HPWRs) zirconium-based alloys have been used for the cladding of the fuel rods and structural components of fuel assemblies for many years, because of their low neutron absorption cross-sections. Two different types of zirconium-based alloys were developed in the middle of the 20th century and are still in use today, in the 21st century. Zircaloy-2 (for BWR application, an alloy with about 1.5% Sn and 0.3% Fe+Cr+Ni) and Zircaloy-4 (with a composition similar to Zircaloy-2 but free of Ni and with a lower tendency of hydrogen Pick-up, for PWR application), were developed in the USA, whereas in the USSR binary Zr-Nb alloy with 1% Nb and 2.5%Nb were selected for the Soviet PWRs and HPWRs. The behaviour of these alloys as fuel claddings and other components has been good over the past decades.

Demanding operational conditions in modern plants and anticipated higher burn-up goals have initiated new development programs for improved corrosion resistance in the last two decades. Zircaloys with optimised microstructure are now being used in BWRs. For PWR application, microstructure and material chemistry of Zircaloy-4 was optimised and alternative zirconium-based alloys with still better corrosion behaviour have been developed. Today several alternative zirconium-based alloys as ZIRLO (1%Sn, 1%Nb and 0.1%Fe), DUPLEX-ELS (a Zircaloy tube with a outer layer with increased Fe+Cr and decreased Sn), Modified Zircaloy-4 (a low Sn Zircaloy with increased Fe+Cr), and M5 (1%Nb 0.12% O) are used for fuel elements in western type PWRs besides optimized Zircaloy-4.

The corrosion of zirconium alloys, however, is still a concern of the utilities and there still occur a number of fuel failures related to fuel cladding accelerated corrosion. The corrosion properties of the zirconium alloys depend on both environment and the material properties as microstructure, material chemistry, and manufacturing process. In one of the ZIRAT-6 special topical reports, the impact of water chemistry on fuel performance, focusing on corrosion properties was discussed. The intent of this special topical report is to provide members with all important aspects related to LWR corrosion performance to allow the utility to implement actions to reduce corrosion. The report covers the range from basic information to current knowledge.

1.1 THE CORROSION ENVIRONMENT

The corrosion performance of zirconium alloys within the core of water cooled reactors depends to a large extend on the corrosion environments. The environmental factors affecting corrosion of Zr alloys are (1) temperature, (2) oxygen respectively hydrogen content of the coolant, (3) additions as boric acid (for a control reactivity), bases (for pH control), and Zn (to keep corrosion of circuit materials and activation of the circuit low), (4) impurities, and (5) products from corrosion of the circuit. Principally, one has to deviate between pressurized reactors with closed cycle (no degassing of the main stream), where formation of oxidative radicals can easily suppressed, and boiling reactors with an open cycle (degassing in a condenser), were oxidative radicals are formed within the core. Table 1-1 summarizes the most important coolant properties within the core of water cooled reactors.

1.1.1 Pressurized-Water Power Reactors (Closed Cycle)

This type of reactor has a core of UO_2, pellets clad in Zircaloy tubes contained in a pressure vessel, through which light water, pressurized by an electrically heated source to 155-158 bar, is circulated to an external steam generator. The core entrance temperature is between 284 and 294°C and fuel assembly outlet temperatures ranges from 300°C to saturation temperature (~345°C). Initially, PWR designated a reactor in which the coolant removed the core energy by forced convective heat transfer. Currently, most PWRs operate with some subcooled nucleate boiling and some PWRs even produce in peak positions modest steam quality. The major elements of the PWR Reactor Coolant System (RCS) are (1) the Reactor Vessel containing an array of fuel rods, (2) two to four steam generators, (3) circulating pumps, and (4) a pressurizer. Water purification and treatment is performed in the PWR auxiliary system, that contains also the Volume Control Tank (VCT), and in case of the Siemens PWRs a degassing system.

The coolant water, which must be compatible with the RCS materials -each with its own corrosion behaviour- is subjecting to a zone of high radiation intensity. The effects of radiation on the coolant are beside radio-activation of water and corrosion products radiolysis of the coolant and unique corrosion problems. Ionizing radiation decomposes water to form the species H^+, OH^-, H, OH, H_2, O_2, H_2O_2, e^-aq and $HO2^-$. The major products are H_2, H_2O_2 and O_2. In nuclear reactor under radiation of pressurized water, the addition of hydrogen or NH_3 reduces O_2 and H_2O_2 concentrations to undetectable levels. Hydrogen is kept in the coolant of the PWRs at 2-4.5 ppm (25-50 cc/kg). According to more recent studies the minimum necessary hydrogen content to suppress oxidative radicals is at about 0.5 ppm (5 cc/kg) e.g. Garbett, et al., 1998 and Christensen, et al., 1996, as can be seen from Figure 1-1. Thus the lower specified value for hydrogen has a significant safety margin. The corrosion potential at O_2 concentrations up to 10 ppb should be out-of-pile between -0.5 to -0.8 V SHE versus Pt. However within the core of a PWR it is higher than in a hydrogenated, oxygen free, and radiation free environment even with >2 ppm hydrogen. According Christensen, et al., 1996 the corrosion potential is about -0.4 V versus Pt, Christensen, et al., 1996, respectively -0.3V versus SS (Figure 1-1). Some plants believe that the optimum H content is in the lower range (between 2.2 and 3.1 ppm), Ishihara, et al., 1998, because increasing hydrogen content increases the Fe solubility and the ratio between ionic Ni and particulate Ni in the coolant. In western type PWRs hydrogen is added and controlled via the cover gas composition of the VCT and in the modern Siemens PWRs via a particular injection system in the auxiliary system. In the Russian WWERs NH_3 is added which decomposes radiolyticaly to N_2 and H_2. In WWERs hydrogen is kept between 2.6 and 5.3 ppm (30-60 cc/kg) and the NH_3 content is typically >5 ppm, Yurmanov, et al., 1997. Also in western type PWRs some NH_3 is often seen if the cover gas in the VCT consists mostly of nitrogen or excess hydrazine is used during start up. Once the ion resins have reached NH_3 equilibrium NH_3 concentrations can reach values up to 2 ppm in the coolant.

In modern PWRs where sub-cooled boiling occurs, some H can be stripped off from the water to the steam bubbles and a local increase of oxidizing species was often suggested. However, Garbett, et al., 1998, has shown that due the high boiling temperature the fraction stripped off is not high enough to initiate oxidative coolant conditions.

PWRs contain boric acid for reactivity control; the concentration is reduced with time during a fuel cycle, usually being near zero at end of cycle. For a twelve month cycle, the initial boron concentration is typically 1,500 ppm but is reduced rapidly over the first few days of the cycle to approximately 900 to 1,200 ppm whilst the xenon and samarium poisons (neutron absorbers) are build up to equilibrium levels in the fuel. Thereafter the boron concentration is reduced approximately linearly at ~ 3 ppm/d. For an 18 month cycle the initial boron concentration is typically 1,800 ppm dropping to 1,500 ppm after a few days. Some PWRs use B10 enriched boric acid. These plants operate with lower total B concentrations. Because acidic coolant conditions result in an increased attack of the circuit materials LiOH, or for Russian WWERs KOH, is added to render the coolant slightly alkaline. LiOH, however can affect corrosion of the Zr alloy cladding as will be shown later.

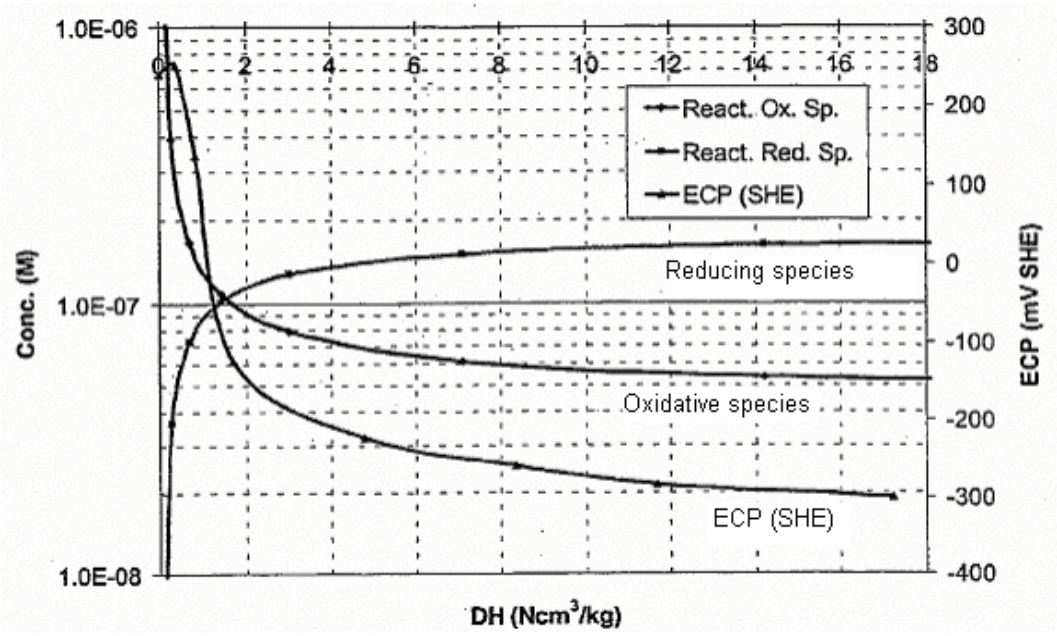

Figure 1-1: Calculated steady-state oxidative species (O_2 and H_2O_2), reducing species (e_{aqu}^-, H), and the SS electrochemical potential versus H_2 content, Christensen, et al., 2000.

The strategy in respect of LiOH has changed over the years. Early specifications only limited the maximum Li content to 2 to 2.2 ppm. In the early 80ies it was recognized that a more constant pH is desirable for reducing the radiation field and fuel depositions. Today, it has been accepted, Wood, 1990, that a minimum pH of about 6.9 (at operation temperature) is required in PWRs to avoid heavy crud deposition on the fuel, which is undesirable for two reasons - fuel cladding oxidation may be accelerated and activation of cobalt in the crud leads to high out-of-core radiation fields from deposition of Co-60. Today the optimum strategy is believed to keep the pH relatively constant between 7.2 and 7.4 and to keep the BOC pH as high as possible. The principle of such a pH strategy has been proven successful for radiation field control for plants with shorter operating cycle's, which require less lithium (≤2.2 ppm) to achieve desired conditions. Recently, several plants with longer operating cycles have raised lithium to the current EPRI maximum recommended concentration of ~3.5 ppm, to achieve an at-temperature BOC pH in the range of 7.1 to 7.2. Current investigations seek to qualify operation at lithium concentrations up to 6 ppm to provide a constant at-temperature pH of 7.4 for modern PWR core designs, Fellers, et. al., 2002. In Figure 1-2 different operational regimes for Li and B are shown.

Recently zinc injection has been implemented in the primary systems of some PWRs, both to reduce primary side cracking of Inconel 600 steam generator tubes (20-50 ppb Zn) and to control dose rates (5-10 ppb), Wood, 2000.

The corrosion product concentration of the PWR primary coolant depends on the materials used for the circuit and steam generator (SG) tubings and on the particular water chemistry of the plant. As material for components and pipe lines austenitic stainless steels are used in western type PWRs, whereas Russian WWERs apply carbon steels. For the SG tubings the Russian WWERs use stainless steel, the Siemens PWRs Incoloy 800, and the other PWRs Ni-base alloy as Inconel 600 and recently Inconel 690. The total Ni content within the water is very low in WWERs (0.01-0.1ppb), moderate in Siemens PWRs (0.02-0,1 ppb), and highest in plants with Inconel 600 SG tubings (normally 0.1-1), Dickinson, et al. 2002.The Ni concentration of PWRs with Inconel 600 SG tubings, however, can vary significantly (probably depending on oxygen, start-up procedure, and temperature) and rich values >>1 ppb.

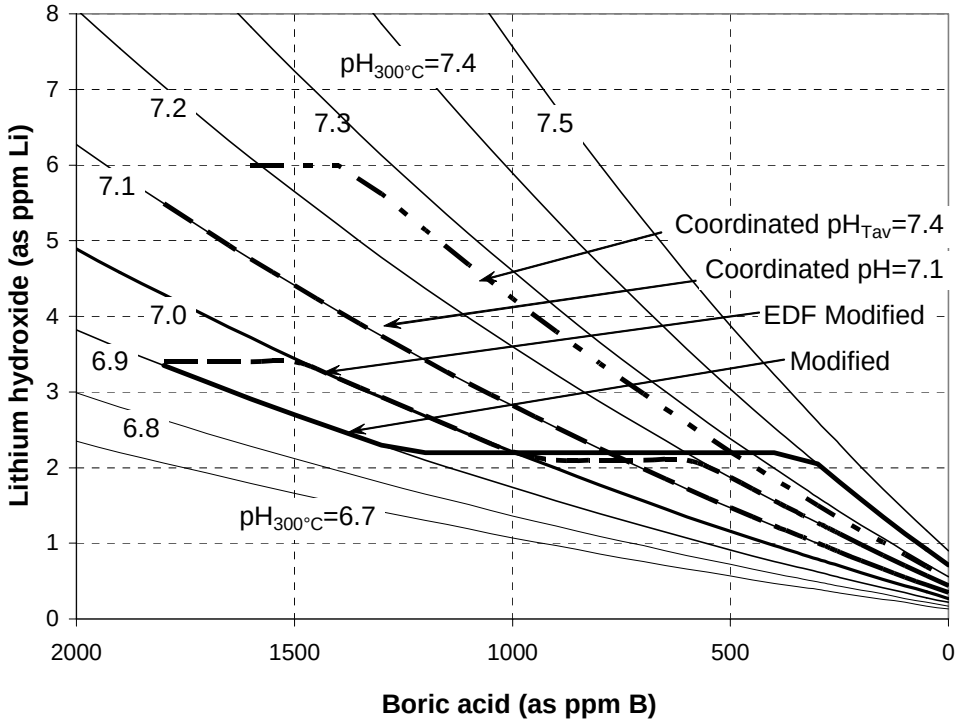

Figure 1-2: Different operational regimes for Li and B.

The Fe content in the coolant is not so different among the different reactor types under optimized coolant conditions. The total Fe content is normally low in Siemens PWRs (0.5-3 ppb) low in WWERs is (0.2-3 ppb) and low in plants with Inconel SG (1-10 ppb) acc., Dickinson, et al. 2002. However it can rich much higher values occasionally depending on coolant conditions. Normally, more than the half of Fe and Ni exists in dissolved form. The particulate fraction of these corrosion products is usually less in a PWR. The corrosion products deposit to a large fraction on fuel rods as CRUD. Highest CRUD loads are generally formed in the upper third, the peak temperature position, of the fuel rods, especially if they experience subcooled boiling. If the corrosion product contains mostly Fe, the CRUD has a low density and consists of relatively loose particles. If, however, the Ni content of the coolant is high the CRUD can become quite dense and may contain boiling chimneys. The fuel rod behaviour is only very little affected by a loose CRUD, can however significantly be affected by a dense CRUD, due to due to higher surface temperatures and concentration of boric acid, lithium hydroxide, and other solutes within the CRUD, as described in detail in chapter 6.1.

More detailed information on PWR water chemistry is given in chapter 4.3

1.1.2 Canada Deuterium Uranium (CANDU) REACTORS (Closed Cycle)

The Canadian pressurised heavy water reactors (CANDU reactors), unlike light water pressure vessel reactors, has a core that comprises of hundreds of small (100 mm) diameter pressure tubes containing natural uranium fuel. The pressure tubes through which the pressurized heat transport system heavy water flows, are separated from each other by a low pressure low temperature heavy water moderator contained in a cylindrical tank called a calandria. The CANDU system contains also SG, a pressurizer and cooling pumps. The later plants have primary coolant boiling in the reactor core with steam qualities up to 4% at the fuel channel outlet.

A deuterium concentration of 3 to 10 cc/kg (0.3-1 ppm H equivalent) is used to reduce dissolved oxygen to acceptable low values.

In the CANDU reactors there is no soluble poison (boron) present in the D_2O**.** Alkalinity is achieved by addition of lithium hydroxide. Table 1-1 shows the typical operation parameters in the primary heat transport coolant. A lithium value of about 1 ppm is added to raise the room temperature pD value to 10.3 - 10.8.

The materials used for modern CANDU reactors are carbon steels for piping and vessel shells and Incoloy 800 or Inconel 600 for SG tubings. The selected materials, primary coolant control, and moderate temperatures result in rather low corrosion product concentrations within the coolant. Furthermore, the fuel element life time is rather short. Thus, not much is reported on CRUD problems in CANDU reactors in spite of the meaning of the word “CRUD”, which stays for Chalk River Unidentified Deposits. The fast flux is also lower in the CANDU reactors.

1.1.3 Boiling Water Power Reactors (Open Cycle)

In this type of reactor, which operates at a system pressure of 70 bars, the reactor core is contained in a pressure vessel through which condensate supplied by a feed pump is circulated by pumps and allowed to boil. The coolant enters the core with a temperature 272 to 278°C and leaves the core as steam water mixture with a temperature of 286°C. The maximum fuel rod surface temperature is at ~290°C. The materials used for pressure vessel cladding, the core internals and the high pressure water lines are stainless steels. Steam is separated from the coolant within the pressure vessel and taken through C-steel pipes to the turbine directly, and then to the condenser which is built up by either by brass, SS, or Ti tubes. The condensate is degassed in the condenser and cleaned in a filter demineralizer or mixed-bed filter. Afterwards heating occurs in low pressure pre-heaters to about 140°C and further on in high pressure pre-heaters to about 220°C. The feed-water heater tubes are mostly austenitic SS while the feed-water shells and feed-water piping are carbon steel. In modern plants, the so-called forward-pumped plants, some fraction of the condensate is returned uncleaned to the feed water line after the low pressure pre-heaters. Under normal water chemistry (NWC) conditions nothing is added to the coolant. Corrosion products from the feed water line, the turbine (in case of partially forward pumped plants), and the condenser, depending on the efficiency of the condensate cleanup system, are entering the reactor. In some reactors Zn (5-10 ppb in the reactor water) is added to minimize plant activation. Some BWRs are operated under hydrogen water chemistry (HWC), where hydrogen is added (1-2 ppm to feed water) for the most part of operation, to reduce the risk of inter granular stress corrosion cracking (ISCC) in structural materials of the water circuit (stainless steels and Inconel). HWC is in some BWRs not effective and has the big disadvantage to increase the activity of the steam significantly. In last years several BWRs have applied noble metal chemistry (NMCA). For NMCA a few kilograms Pt and Rh are added during a reactor shut down (with the goal to be plated out over the whole surface of the construction parts) and a small amount of hydrogen during the most time of operation. NMCA is believed to be more efficient to mitigate ISCC and needs less hydrogen addition. It therefore increases steam activity less than HWC.

Pressure, max operation temperatures of Zr-alloy components, and fuel rod heat fluxes are lower in BWRs than in pressurized water reactors, as shown in Table 1-1. Typical water chemistry data are given in Table 1-2.

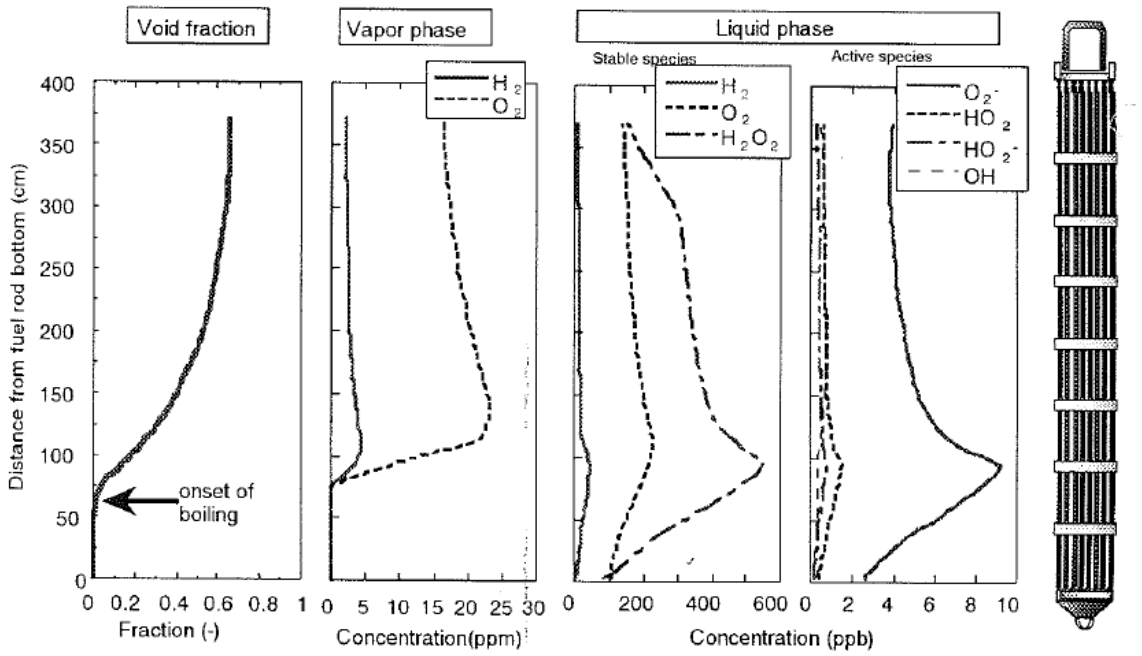

Figure 1-3: Calculated profile of radiolysis species along a fuel rod in a BWR 4 type reactor during NWC, Nishino, et al., 1998.

BWR are normally open cycle reactors with direct connections between the reactor and the turbine in the steam system, the condenser and the reactor in the feedwater system. If nothing is added, an oxygen content of 125-500 ppb is measured in the reactor coolant in the water sample line before the reactor cleanup system and 20-30 ppm in the steam. This oxygen is formed by radiolysis in the water phase within the core due to stripping off of the hydrogen. In early closed cycle BWRs the oxygen in the reactor coolant had reached equilibrium values of 1000 to 2000 ppb. As calculations indicate Figure 1-3 the oxygen content within the fuel rods may be even less than in the rector water before the reactor clean up system, however, short living radical species, especially H_2O_2, may reach quite high concentrations within the fuel element. These oxidizing radicals decompose after leaving the core to O_2 increasing the oxygen content of the reactor coolant in a short time. At the position of the reactor sampling line before the reactor cleanup system the H_2O_2 concentration is usually very low. The corrosion potential in a water with 300 ppb oxygen would be out-of-pile at 0 to 0.1 V, SHE. Within the core of BWRs with NWC even higher values have been found (0.1 to 0.3 V, SHE), what reflects the high red/ox potential of the H_2O_2, Indig M. E., 1989.

Under HWC the profile of the radiolytic species changes with increasing H addition between the fuel rods especially in the lower part and in the water bypass between the channels respectively within water rods over the whole length, as can be seen from Figure 1-4. As obvious in the boiling channels H additions can not suppress radiolytic formation of oxidizing radicals due to the fact that all H is stripped off to the steam. Electrochemical measurements in BWRs under HWC have shown a significant reduction of the corrosion potential only in the bypass channel whereas in the boiling channel a significant reduction was only seen in the lower part, Indig M. E., 1989.

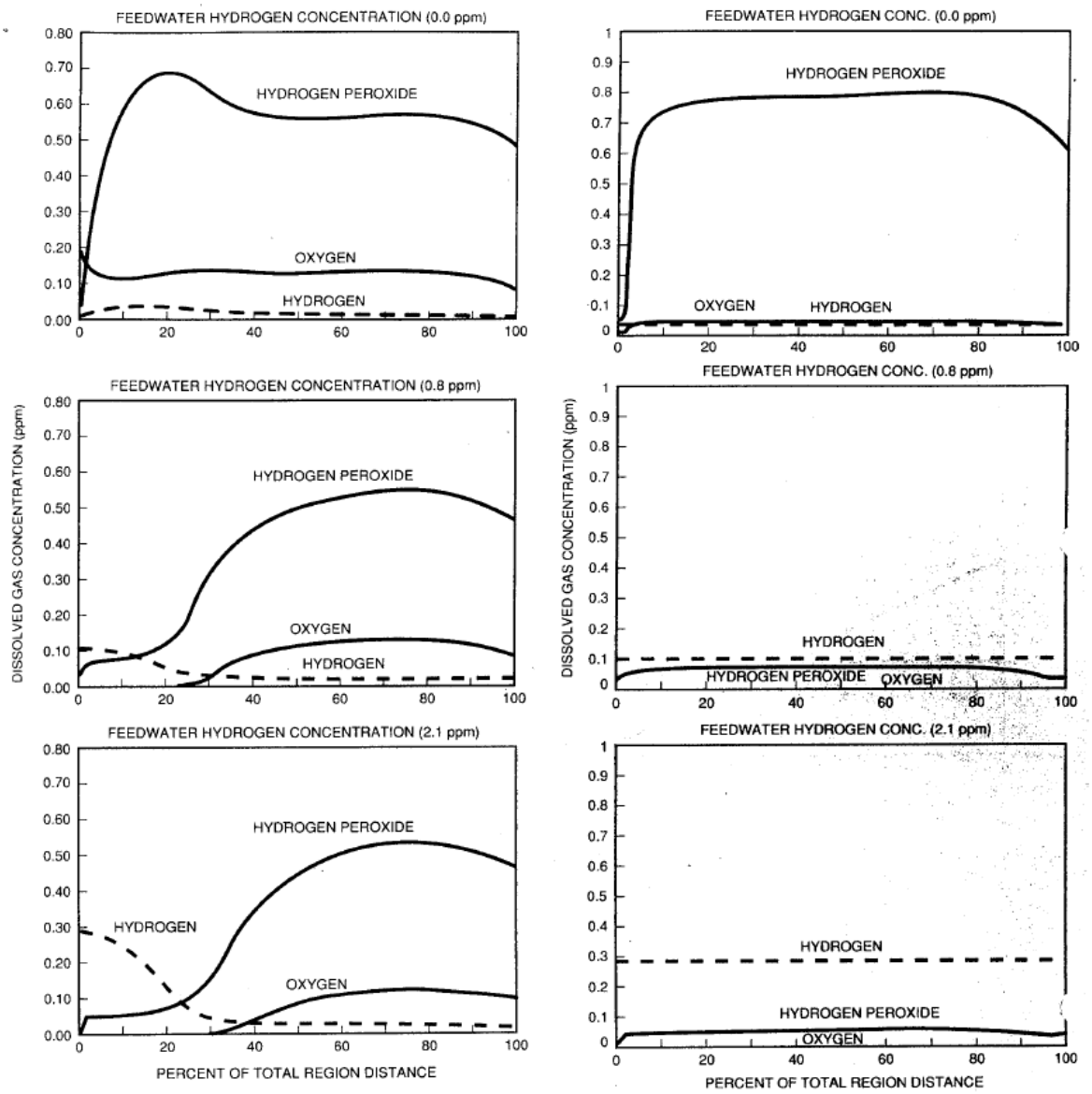

a) Aqueous fuel channel b) Bypass channel

Figure 1-4: Calculated profile of radiolysis species along a fuel rod in a BWR reactor during HCW for different H additions to the feedwater, Ruiz, et al., 1989.

Another species which was found to influence Zircaloy corrosion is nitrogen, Shimada, et al., 1997. Nitrogen was reported to have a concentration of 30 to 800ppb in the reactor water, Garzarolli and Stehle, 1986. Nitrogen can enter via the feedwater line (8-14% of total core flow) if air-saturated makeup water is added and air leaks in through the condenser. Furthermore, sometimes air saturated water is used for the sealing water of the control rod drives (≈0.15% of feed water) and coolant pumps (≈0.2% of feed water). These numbers can vary significantly from BWR to BWR.

High concentrations of sulphate, nitrate and sodium-hydroxide can result even in fuel cladding corrosion defects if released from the demineralizer resins in larger concentrations, Kobayashi, et al., 1997. The release rate depends on cleanup system, operation temperature, resin treatment, and type of resin (for more details see chapter 6.2).

Corrosion products may affect the corrosion of Zircaloy claddings via a local increase of the temperature after deposition, by a chemical influence, and probably also by an electrochemical effect. The corrosion product concentration entering through the feedwater (FW) line depends on the construction materials applied and the FW treatment. A significant fraction of the Fe is coming from the FW shells and piping which are carbon steels. To keep this fraction of the Fe corrosion products low the oxygen in the FW line should be kept between 20 and 200 ppb. The total Fe content of the FW can reach several ppb, especially in forward pumped plants, but it can also be significant below 1 ppb in other plants. Most of the Fe is present in the reactor water as fine particles, whereas a substantial fraction of Ni and most of the Cu, Zn and Cr is soluble. Most of the corrosion products deposit on the surface of the fuel assemblies. These deposits (CRUD) preferentially contain iron and in some plant in addition a high portion of copper. Thickest CRUD layers are generally observed in the lower part of the fuel assembly where boiling starts. The Fe rich CRUD layers have a low density and therefore do no affect heat transfer from the fuel rod to the coolant. Much more critical are high concentrations of soluble species like copper. They can form a dense CRUD layer which can result in a local break down of the heat flow and, as a consequence, in CRUD induced localised corrosion (CILC) defects (see section 6.1.3).

The type of the CRUD layer oxide formed is very much determined by the balance between Fe and bivalent metal ions such as Ni, Cu and Zn. In plants with a relatively high Fe content the structure of the particulate corrosion products is usually hematite (α-Fe_2O_3). In plants with a rather low Fe content the impurity content of the bivalent Ni or Zn-additions can stabilize spinels ($NiFe_2O_4$ or $ZnFe_2O_4$). The ratio between spinel and hematite increases significantly with Zn additions, Levin and Garca, 1995. In plants were Fe/(Ni+Zn) <2 (iron deficient water chemistry) even NiO or ZnO may form in addition. Under this conditions, the solute content of bivalent species will increase because the solubility of the bivalent metal oxides are larger than the solubility of the spinels. When comparing cladding performance in different reactors and during different time periods in the same plant, a strong correlation between enhanced spacer shadow corrosion (normally shadow corrosion saturates with burnup, whereas ESSC accelerates at high burnup, as discussed detailed in chapter 6) and iron deficient water chemistry was identified, Zwicky, et al., 2000.

More detailed information on BWR water chemistry is given in chapter 4.3.

1.1.4 Boiling Pressure Tube Power Reactors

The BWRs which use heavy water, as the SGHWR and, or graphite as moderator and light water as coolant, as the Russian BRMK reactors, and service medium (steam) can be considered from chemical viewpoint as similar with the typical light water BWR. However they have a lower power rating and neutron flux. The operating data for RBMK reactors are given in Table 1-1.

Table 1-1: Design Parameters-Water-Cooled Reactors.

Parameter	**Western type PWR**	**WWER (440/1000) MW**	**CANDU**	**BWR**	**RBMK**
1. Coolant	Pressurized H_2O	Pressurized H_2O	Pressurized D_2O	Boiling H_2O	Boiling H_2O
2. Fuel Materials (Pressure tube materials)	Zry-4, ZIRLO, DUPLEX, M5, Inconel, SS	Zr-alloy E110	Zry-4 (Zr2.5Nb)	Zry-2, Zry-4, Inconel, SS	Zr-alloy E110, (Zr2.5Nb)
3. Average power rating, (kW/l)	80-125	83/108	9-19	40-57	5
4. Fast Neutron Flux, Average, n/cm².s	6-9E13	5E13/7E13	1.5-2E12	4-7E13	1-2E13
5. Temperatures, °C					
Average Coolant inlet	279-294	267/290	249-257	272-278	270
Average Coolant outlet	313-329	298/320	293-305	280-300	284
Max Cladding OD	320-350	335/352	310	285-305	290
Steam mass content, %				7-14	14
6. System pressure, bar	155-158	125/165	96	70	67
7. Coolant Flow, m/s	3-6**	3.5/6	3-5	2-5**	3.7
8. Coolant Chemistry					
Oxygen, ppb	<0.05	<0.1		200-400	<20
Hydrogen (D_2), ppm	2-4		(3-10)	See text	-
cc/kg	25-50	30-60			
Boron (as Boric acid), ppm	0-2200	0-1400	-	-	-
Li (as LiOH), ppm	0.5-3.5	0.05-0.6	1	-	-
K (as KOH), ppm	-	5-20		-	-
NH_3, ppm		6-30			
NaOH, ppm		0.03-0.35			

** Variation from lower to upper part of the core and from plant to plant

Table 1-2: Water Chemistry of BWR Plants.

Parameter		**Optimum,** Cowan, 2000	**Current av.,** Cowan, 2000; IAEA-Symposium, 1982 and IAEA-Symposium, 1993
RW-ECP	mV-SHE	≤-230	+100 to +300[(1] / ≤-230[(2]
RW-Sulphate	ppb	<5	~1
RW-Chlorate	ppb	<5	~2
RW-Conductivity	µS/cm	<0.08	0.095
RW-Total Fe	ppb		0.2-10
RW-Total Cr	ppb		1-2
RW-Total Ni	ppb		0.1-0.5
RW-Total Cu	ppb	<0.5	0.3-15
RW-Total Zn	ppb	5-10	0.1-3 / (5-10)[(3]
RW-SiO_2	ppm		<0.1-1
FW-Conductivity	µS/cm	<0.065	0.058
FW-Total Fe	ppb	0.5-1.5	<0.1-3
FW-Total Ni	ppb		<0.1-0.3
FW-Total Cu	ppb	<0.05	<0.1-0.5
FW O-content	ppb	20-50	20-100
FW H-Addition	ppm	yes	No[(1] / 0.8-2[(2] / 0.15-0.4[(4]

[(1] NWC, [(2] HWC, [(3] in plants with admiralty brass condenser tubes respectively in plants with Zn additions, [(4] NMCA

1.2 HISTORY OF ZIRCALOYS

Zirconium was discovered in 1824 by Berzelius. In 1925 Van Arkel and de Boer developed the iodide process for refining zirconium and produced high purity “crystal bar” zirconium. In 1947 the U.S. Bureau of Mines developed the zirconium sponge process. After 1948 when the low neutron absorption characteristics of Zr was established, a considerable effort was made to develop Zr alloys particularly for use in water cooled reactors and in1949 its combination of mechanical properties and low neutron absorption cross section resulted in its being selected as the structural material for the nuclear reactors of submarines. Since the late 50ies respectively early 60ies Zr alloys have been used for the fuel elements of BWRs and PWRs.

Unalloyed Zr exhibits an excellent corrosion resistance in oxygen by forming a thin black very protective oxide layer. Corrosion rate of Zr in oxygen follows an almost parabolic rate law with low rates at least up to 425°C. However in 300 to 400°C water and steam formation of a white non-adherent oxide was observed after some time depending on temperature and material purity, particularly the N content, Kass, 1962. This phenomenon was called break away and did forbid the application of pure Zr for water cooled reactors. The subsequent zirconium alloy development program had the goal to search for an alloy which would behave in water in the nearly identical manner as observed for pure zirconium in oxygen. It was found that additions of Sn counteract the deleterious effect of N but decrease the general corrosion resistance of Zr and that additions of Fe, Cr, and Ni improve the corrosion resistance of Zr-Sn alloys. The first commercially used alloy was Zircaloy-2 which contains beside 1.5% Sn small additions of Fe, Cr, and Ni (together 0.3%) as can be seen from Table 1-3. This alloy was developed in the USA, Kass, 1962, and is still used for BWR fuel elements today. Later it was shown that Zircaloy-2 picks up a quite large fraction of the corrosion hydrogen in oxygen-free and hydrogenated water what can result in an embrittlement after long-time service. The alloying element Ni was found to be responsible for the large pick up fraction. As consequence Zircaloy-4 was developed, which is similar as Zircaloy-2 but has replaced Ni by Fe, as can be seen from Table 1-3. Zircaloy-4 is still in use for PWR fuel elements today.

In Russia a similar exploratory program was performed with Zr alloys. For commercial application a Zr alloy with 1%Nb was developed for fuel rod claddings and an other Zr alloy with 2.5%Nb, with a higher strength, for the pressure tubes of their RBMK reactors (see f.i., Ambartsumyan, et al., 1958). Zr2.5%Nb is also used for the pressure tubes of the CANDU reactors.

Zircaloy-2 claddings for BWR fuel were improved over the years to overcome specific phenomena resulting from BWR applications. A soft inner liner was introduced in 1984 to avoid the so-called "pellet cladding interaction" defects. For prevention of the so-called "crud-induced localized corrosion" defects, the resistance against nodular corrosion was optimized between 1984 and 1990. In recent years emphasis was placed on the improvement of the behavior of defective fuel rods during continued irradiation. Today, investigations concentrate on two issues, the anticipated increased burnups and new water chemistries such as noble metal addition, Garzarolli, 2001.

PWR claddings were improved over the years mainly in respect of their corrosion resistance to allow increased burnups and optimized loading strategies. In the first phase, which started in 1988, Zry-4 corrosion performance was improved by: 1) lowering the target Sn-content, 2) tightening the chemical composition and, 3) optimizing the microstructure. During the second phase, which started in 1990, Zr alloys with a composition outside of Zircaloy-4 such as DUPLEX ELS, ZIRLO, modified Zry-4, and M5 were applied for reloads of high burnup fuel of thermal-hydraulically demanding PWRs. Today, the investigations particularly concentrate on the increasing maximum power densities., Garzarolli, 2001.

Table 1-3: Chemical composition of Zr alloys used for water cooled power reactors.

Alloy	**Sn (%)**	**Nb (%)**	**Fe (%)**	**Cr (%)**	**Ni (%)**	**O_2 (%)**
Ziraloy-2	1.5		0,14	0.1	0.05	0.13
Ziraloy-4	1.5		0.22	0.1		0.13
Alloy E110		1.0				
Alloy E125		2.5				
ZIRLO	1.0	1.0	0.1			
DUPLEX -ELS Base Outer layer	 1.5 0.5-0.8		 0.2 >03	 0.1 >0.15		 0.13
M5		1.0				0.12

1.3 FORMS OF CORROSION OBSERVED

The different types of corrosion observed for Zircaloy in water out-of-pile and in-pile are listed in Table 1-4. Under out-of-pile exposure in high temperature water and steam, Zr alloys form initially a thin black and adherent oxide film. Pure Zr samples show often a sudden rapid increase in the corrosion kinetics (coincident with the formation of a white corrosion product). Shortly after this so called "Break away" spalling and flaking of the oxide occurs. The time to break away varies significantly from sample to sample. The variations have been correlated to the content of the impurity nitrogen, Kass, 1962. In Zircaloys and other Zr alloys a rate transition from an early cubic to an almost linear behaviour occurs at an oxide layer thickness of about 2 to 3 µm without loosing adherence. The time to transition as well as the linear post transition corrosion rate can be well described by an Arrhenius law, const · exp(-Q/RT), applying an "activation temperature Q/R" of 12,000 to 16,000 K, Garzarolli, et al., 1988.

Irradiation has an accelerating effect on corrosion of Zr alloys. Important parameters for this effect are the hydrogen and oxygen content of the water. According to Cox, 1985, below a H/O ratio <1 (BWR conditions) corrosion increases from the beginning. BWR fuel elements with Zircaloy and alloy E110 cladding and structural components show uniform oxide layer formation which is much thicker than expected from out-of-pile testing. After about 100 days a thickness of 2 µm is formed which increases at long operation times to 10-20 µm. Furthermore, often a non-uniform type of corrosion is formed after some incubation time which is called nodular corrosion. This type of corrosion is characterized by the formation of irregularly shaped patches of thick oxide which increase in depth and spread during prolonged exposure. The nodules can grow together and then form thick and practically uniform oxide films. At high exposure times nodular oxide layer thicknesses of >100 µm can occur. In visual inspection the oxide patches appear as white spots. The number density of the nodules in general stays constant after the first nucleation. The tendency to nodular corrosion depends on the microstructure of Zircaloy, especially the size and distribution of the second phase particles (SPP) and can be simulated out-of-pile in high pressure (>70 bar) steam at ≥500°C, e.g., Garzarolli and Holzer, 1992. A general observation in the core of BWRs is an increased corrosion of Zircaloy in the area of Inconel spacers, Inconel springs, and stainless steel components. This type of corrosion is called shadow corrosion (for details see chapter 6.2) and is formed early in life and does not normally increase any further at higher burnups, see section 6.2. However in one recent case in KKL, the shadow corrosion accelerated at higher burnups leading to fuel failures. This type of corrosion is called shadow corrosion, (ESC). In fine gaps some kind of crevice corrosion can form in addition. At high neutron fluences an increase of corrosion is observed for Zircaloy claddings with fine SPP, e.g., Garzarolli, et al., 2001(a). It is proposed that this increase is due to irradiation induced dissolution of the SPP. For Zircaloy-2 claddings with fine SPP, an increased hydrogen pickup is reported in addition, Tägström, et. al., 2001. If the H content in the cladding exceeds the terminal solubility, a dense hydride rim can form at heat fluxes >50 W/cm², e.g., Garzarolli, et al., 2001(a). A dense hydride rim will cause a further increase of corrosion. Figure 1-5 indicates the time dependency and relative thickness for the different types of corrosion observed in a BWR.

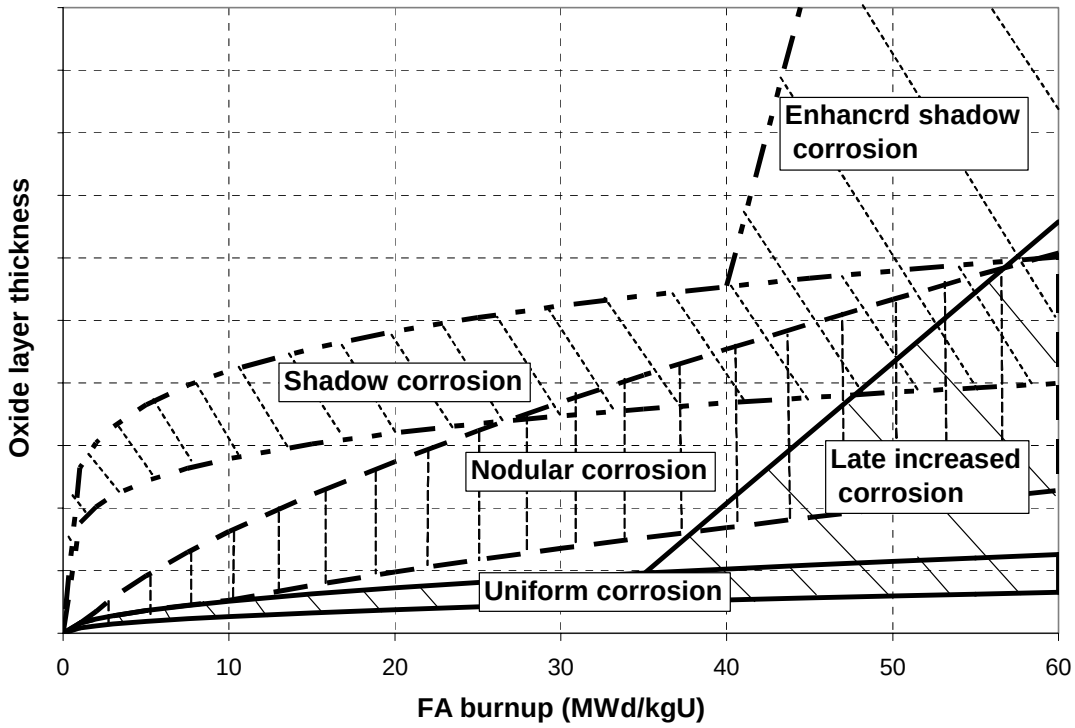

Figure 1-5: Characteristics of the different types of corrosion observed in BWRs.

In difference to BWRs, no or only little effect of irradiation on the corrosion behavior of Zr alloys is seen under hydrogenated coolant conditions, e.g. in PWRs, as long as the oxide layer thickness is low or moderate. After a certain oxide layer thickness uniform corrosion rate is increased due to irradiation. The uniform corrosion rate increases with increasing temperature in-PWR similar to that observed out-of-pile. Zircaloy claddings with fine SPP often exhibit an (only little temperature but largely flux dependent) increased corrosion. In low Sn Zr alloys hydrogen pickup can be quite high. This can at large heat fluxes result in a noticeable increase of corrosion above a certain oxide layer thickness (once a dense hydride rim has formed due to the thermal redistribution of the hydrides to the cooler outer side). Furthermore, if fast neutron fluence exceeds 1E22 (n/cm^2, $E \geq 1MeV$) the corrosion may increase significantly due to an still unknown mechanism, Garzarolli, et al., 2001(a). For normalization of the oxide layer measurements often the fuel rod burnup is often used. However, this allows reasonable conclusions only if the thermal operating conditions are equivalent. Other possibilities to normalize corrosion are the exposure time, which is mostly less meaningful than the burnup, the “Temperature Normalized Time”, proposed by Garzarolli, et al., 1996b and the “Fuel Duty Index”, proposed by Kaiser, et al., 2000, see section 5.3.1.

Much more detailed information on the forms of corrosion and the ways of evaluation is given in chapters 3 and 4.

Table 1-4: Types of corrosion observed with Zircaloy in-reactor and out-of-pile in water.

Type of corrosion	**Comment**	**Observed**	**Irradiation effect in oxygenated coolant (BWR)**	**Irradiation effect in hydrogenated coolant PWR**
Uniform	Normal mode	Out-of-pile, in-BWR and, in-PWR	5-10x increased from beginning, low flux dependency	2-4x increased after 1st corrosion rate transition, low flux dependency
Nodular	Local break down of oxide protectivness	In-BWR and out-of-pile>500°C, Zry with large SPP	Increases almost linear with fast flux, little temp. dependency	not observed
Shadow corrosion	Probably driven by potential differences	Only under irradiation and oxidative coolant conditions (BWR)	Increases probably almost linear with fast flux	not observed
Crevice corrosion	Change of environment in small gaps	Out-of-pile, in-BWR and, in-PWR	observed	Observed
Increased corrosion with fine SPP	Reduction of protectively	Out-of-pile, in-BWR and, in-PWR	Increases almost linear with fast flux	Increases almost linear with fast flux, little temp. dependency
Increased corrosion at high fluences	Reduction of protectively	In-PWR	?	Increases with increasing fluence above a critical threshold
Increased corrosion at high hydride concentrations	Lower corrosion resistance of hydride	Out-of-pile, in-BWR and, in-PWR	observed	Flux dependent but less temperature dependent

2 CURRENT ALLOYS AND THEIR MICROSTRUCTURE (F. GARZAROLLI)

2.1 COMMERCIAL AND EXPERIMENTAL ALLOYS

Initially Zircaloy-2 was used for the claddings of BWR fuel and Zircaloy-4 (respectively E110) for PWR fuel rods. The specified composition is given in Table 2-1. The fabrication process of the early claddings was tailored to meet the requirements of the available production capabilities of the various suppliers. Later on fabrication and chemistry was optimized for improved in-reactor performance.

The materials of interest for BWR and PWR application are listed in Table 2-1. The experimental alloys can be subdivided in (1) Zr alloys with transition metals Fe, Cr, Ni and V, (2) Zr-Sn-Nb alloys with transition metals Fe, Cr, Ni and V, (3) Zr-Sn-Nb alloys without transition metals additions, (4) Zr-Nb alloys, and (5) other Zr alloys with Cu, Mo, Te, Bi, and Ta.

More information on the different Zr alloys is given especially in the chapters 4, 7, and 8.

2.1.1 PWR Cladding Materials

The major objective of PWR cladding development was to improve fuel element economy, to allow a higher burnup and local power density. For this purpose it was necessary to improve the corrosion resistance of the fuel rod cladding. In a first phase, tests were performed on Zircaloy-4 cladding with varying alloying content, impurity content, and material condition, to optimize the corrosion behavior. These tests showed that Sn, C and Si influence corrosion in PWRs. As result, a Zircaloy-4 cladding with a restricted chemistry, the “low-Sn-Zry-4”-cladding, has been specified and applied for reloads since 1988, e.g., Garzarolli, 2001. Further tests revealed that the transition metal alloying content and the microstructure also have a pronounced effect on corrosion. Applying these results it was possible to develop the “optimized Zry-4”, with Fe in the upper range of the ASTM specification and an optimized microstructure. This type of cladding, which is somewhat different specified by the different vendors, has been used for reloads after 1989 and is still in use for moderate operating conditions today, e.g., Garzarolli, 2001.

It was concluded in the early 80ies that even the best Zry-4 does not permit achievement of the final burnup target in modern PWRs. Therefore, in a second phase several promising alternative Zr alloys were examined with test fuel rods and corrosion coupons in water rods in PWRs. The following alloying systems were tested in different programs:

Zr 0.2-1.2%Sn 0.1-0.7%Fe 0-0.7%Cr 0-0.3%V

Zr 0.2-1%Nb 0.2-0.6%(Fe+Cr+V)

Zr 0.2-1.5%Sn 0.2-3%Nb 0-1%(Fe+Cr+V)

Zr 0.5-2.6%Nb

Zr 0.5-1.1% (Fe+Cr+V)

The different fuel suppliers selected different cladding materials for their advanced fuel elements. The first new type of cladding that was used for reloads in 1988/89 is the DUPLEX (DX) cladding. This type of cladding consists of a Zircaloy-4 tube with a metallurgical bonded extra-low Sn (ELS) outer layer, about 100 μm thick, and is stress relieved. The outer corrosion-resistant layer has a Sn level below, and Fe and Cr levels above the range specified by ASTM for Zry-4. This cladding has been used commercially only for European PWRs operating under very demanding conditions. ZIRLO is the other alternative Zr-alloy cladding that was introduced in the market in the late 80ies. The alloy is a Zr alloy with about 1%Sn, 1%Nb and 0.1% Fe and is based on the E636 alloy, Amaev, et al., 1971, developed in Russia. Although stress relieved, it has high creep strength due to the relatively high solute content of Sn and Nb, a good out-of-pile resistance to LiOH, and a slightly better corrosion behavior in PWR than Zircaloy-4. It has been used commercially especially for the fuel Elements of the Wesinghouse type PWRs. To fulfill the demands of the market, the supplier reduced the Sn content of the alloy at least once, Comstock, et al., 1996. The corrosion resistance of ZIRLO is probably not better than that of Optimized Zircaloy-4. Therefore, ZIRLO must be improved further to meet the future demands. In 1995 the partially recrystallized “modified Zircaloy-4” with an enhanced Fe+Cr content (above the ASTM range for Zircaloy-4) was applied for reloads in European reactors with “moderate” thermal hydraulic conditions. This material has the same mechanical behavior as Zircaloy-4 but a superior corrosion behavior, e.g., Garzarolli, 2001. In 1996 the M5 alloy was introduced in the market on a commercial basis. M5 is a fully recrystallized ternary Zr1Nb0.125O alloy and was developed in an extensive irradiation program starting in 1989, Mardon, et al., 2000. It is an advancement of the Russian E110 cladding material. This alloy is proven to have a high creep resistance, a high corrosion resistance, and a low hydrogen pickup fraction and is used today for reloads all over the world. The large number of examinations performed has shown that M5 is equivalent or even better than Zircaloy-4 with respect to accident considerations, Mardon, et al., 2000. To provide materials for future still more demanding operation conditions, advanced Zr alloys including ZrNb- and ZrSnFeV-alloys (as HPA-4) have been tested since the mid-eighties in different reactors under the most demanding conditions to very high burnups. This program has shown promising results for the corrosion behavior of DX Zr2.5Nb and HPA-4, e.g., Garzarolli, 2001. Additional in-PWR tested materials, which were however never applied commercially, are reported in Mardon, et al., 1994(a); Garde, et al., 2001, and Besch, et al., 1996. In out-of-pile tests for PWR cladding development many additional alloys have been tested. Recently the effects of Cu and Ta on the corrosion behavior of 1.0% Sn Zircaloy-4 and Zircaloy-2 type alloys were reported, Takeda and Anada, 2001. Best corrosion out of pile behavior was seen for alloys with 0.1-0.2% Cu and Ta additions.

See also sections 4.4 and 7.2 for more information.

2.1.2 BWR Cladding Materials

For many years the major objective of the development of BWR claddings was to avoid fuel failure. In the last decade emphasis was placed on the anticipated increased burnups and new water chemistries. The corrosion behavior of Zircaloy for BWR was optimized in respect to the second phase particle (SPP) distribution in the early 80ies. In the early 60ies, when Zircaloy-2 and -4 in the USA and E110 in Russia were selected for BWR applications it was doubted that the alloy could fulfill future demands. Therefore alternative Zr alloys were considered. In the late sixties experimental alloys such as Zr1.2%Cr0.1%Fe (Valloy) and Zr1%Sn3%Nb were tested in experimental fuel assemblies in USA and Germany. In Russia the alloys Zr2.5%Nb, Zr2.5%Nb0.5%Cu, Zr1%Sn0.5%Fe, Zr0.7%Fe0.7%Ni, and Zr1%Sn1%Nb0.5%Fe were tested in comparison with Zr1%Nb, Amaev, et al., 1971. However, because of the excellent experience with the originally selected alloys (e.g. Zircaloy-2) further research of alternative alloys was neglected for many years. In the late 80s, attention focused again on alternative alloys. New in-BWR corrosion sample irradiation programs were started in several reactors in Germany, the US, and later also in Japan. The results of these irradiation tests are reported in Etoh, et al., 1996; Ishimoto, et al., 2000 and Garzarolli, et al., 2001(b), for exposure times up to 1200-1600 days. The tests revealed that Zry-2 is an excellent alloy. The transition metal content has accordingly little influence on in-BWR corrosion although it has a pronounced effect on out-of-pile behavior in 500°C steam. Increased corrosion has been experienced with Sn contents <1% and >2%, with Nb additions and Mo additions to Zry-2, for ZrSnNbMo, ZrSnNbFe, ZrSnNbTe, ZrSnTe, ZrNbBi and binary ZrNb alloys. A low corrosion was reported only for Zry-2 type alloys with increased Fe and for Zr1Sn3Nb, e.g., Etoh, et al., 1996; Ishimoto, et al., 2000 and Garzarolli, et al., 2001(b).

See also sections 4.4 and 7.1 for additional information.

Table 2-1: Composition of Commercial and Experimental Alloys.

Alloy	Sn %	Nb %	Fe %	Cr %	Ni %	O %	Others alloy elem.	%	Ref.
1. Commercial alloys									
Zircaloy-2	1.2-1.7	-	0.07-0.2	0.05-0.15	0.03-0.08	0.1-0.14	-	-	ASTM
Zircaloy-4	1.2-1.7	-	0.18-0.24	0.07-0.13	-	0.1-0.14	-	-	ASTM
E-110	-	0.9-1.1	0.014	<0.003	0.0035	0.05-0.07	-		Shebaldov, et al., 2000
Alloy E125	-	2.5	-	-	-	0.06	-		Solonin, et al., 1999
Zr2.5Nb	-	2.4-2.8	<0.15	-	-	0.09-0.13	-		ASTM
ZIRLO	1	1	0.1	-	-		-		Comstock, et al., 1996
DX-ELS-Liner	0.5/0.8	-	0.3/0.5	0.2	-	0.12	-		Garzarolli, 2001
PCA-2b	1.3	-	0.3	0.2	-		-		Garzarolli, 2001
M5	-	0.8-1.2	0.015-0.06	-	-	0.09-0.12	-		Mardon, et al., 2000
2. Experimental alloys									
Zircaloy-1		2.5	-	-	-		-		Cox, et al., 1998
Zircaloy-3A	0.25	-	0.25	-	-		-		Cox, et al., 1998
Zircaloy-3B	0.5	-	0.4	-	-		-		Cox, et al., 1998
Zircaloy-3C	0.5	-	0.2	-	0.2		-		Cox, et al., 1998
Zr1Sn0.5Fe	1	-	0.5	-	-	0.1	-		Amaev, et al., 1971
ZrSnFe	1.3-1.5	-	0.26-0.3	<0.05	-		-		Garzarolli, et al., 2001(b)
M4	0.5	-	0.6	-		0.12	V	0.3	Mardon, et al., 1994(a)
D2	0.5	-	0.4	-	-	0.1	-		Besch, et al., 1996
High Fe Zry-2	1.5	-	0.26	0.10	0.05		-		Ishimoto, et al., 2000
HighFeNi Zry-2	1.4	-	0.26	0.10	0.10		-		Ishimoto, et al., 2000
ZrSnFeO	0.5	-	0.4	-	-	0.22	-		Garde, et al., 2001
Alloy-C	0.4	-	0.5	0.24	-	0.18	-		Garde, et al., 2001
HPA-4	0.4-0.6	-	Fe	-	-		V		Seibold, 2001
Valloy	-	-	0.15	1.2	-	-	-		Cox, et al., 1998
Zr.7Fe0.7Ni	-	-	0.7	-	0.7	0.03	-		Amaev, et al., 1971
Zr0.25Fe0.2V	-	-	0.25	-	-		-		Cox, et al., 1998
E635	1.1-1.4	0.9-1.1	0.3-0.5	-	-	0.05-0.07	-		Solonin, et al., 1999
Alloy-A	0.5	0.3	0.35	0.25	-	0.15	-		Garde, et al., 2001
Alloy-E	0.7	0.4	0.45	0.24	-	0.13	-		Garde, et al., 2001
NSF 0.2	1	1	0.2	-	-	0.1	-		Cox, et al., 1998
T18/I18	1	0.6	0.2	-	0.05		-		Etoh, et al., 1996
NSF 0.5	1	1	0.5	-	-	0.1			Etoh, et al., 1996
Zr3Nb1Sn	1	2-3	-	-	-		-		Garzarolli, et al., 2001(b)
Ozhenite 0.5	0.2	0.1	0.1	-	0.1		-		Cox, et al., 1998
M3	0.5	0.5	0.25	-	-	0.12	-		Mardon, et al., 1994(a)
0.2 Nb Zry-2	1.5	0.2	0.15	0.10	0.06		-		Etoh, et al., 1996
0.5 Nb Zry-2	1.5	0.5	0.15	01	0.05		-		Ishimoto, et al., 2000
D3	1.4	1	0.2	0.1	-		-		Besch, et al., 1996
EXCEL	3.5	0.8	-	-	-		Mo	0.8	Cox, et al., 1998
XXL	1.2	0.3	-	-	-		Mo	0.3	Ishimoto, et al., 2000
T12-15/I12-15	1	1-2	-	-	-		Mo	0.2-0.5	Etoh, et al., 1996
T19/I19	1.4	0.4	-	-	-		Te	0.2	Etoh, et al., 1996
T20/I20	1.2	-	-	-	-		Te	0.6	Etoh, et al., 1996
BAG	-	0.5	-	-	-		Bi	1	Ishimoto, et al., 2000
T68	0.8	-	0.3	0.1	0.1		Cu/Ta	0.2/0.2	Takeda and Anada, 2001
T40	1	-	0.25	0.1	-		Cu/Ta	0.1/0.2	Takeda and Anada, 2001

2.2 PHASE DIAGRAMS APLICABLE TO COMMERCIAL ALLOYS

Pure Zr has at low to moderate temperatures a hexagonal closed packed (hcp, a=3.23 Å and c= 5.15Å) crystal structure (α-Zr) and at high temperatures a body centered cubic (bcc, a= 3.61Å) crystal structure (β-Zr). The melting point of pure bcc zirconium has been accepted as 1852°C and the α/β-transformation temperature as 863°C. α Zr has an anisotropic behavior. The thermal expansion of in the c-axis [0001] direction is almost 2 times higher than of the a-axis. The mechanical properties and diffusion have also an anisotropic behavior.

Alloying elements in solute solution change the lattice parameters, depending on the atomic size of the solute and the mode of solid solution (substitutional or interstitial). If the thermal solubility is exceeded, second phase particles (SPP) appear. The solute alloying content and the SPP can affect the microstructurel, mechanical, and corrosion behavior.

Zirconium has a particularly high affinity for certain non-metals, as O. This and the tendency to take these elements in solid solution render its refining, necessary for binary phase diagram studies, difficult. However, for practical interests truly binary systems are rather academic. For practical purposes, even tentative diagrams are quite useful.

In Table 2-2 the most interesting parameters, as atomic no. and weight, neutron cross section, atom size and misfit, solubility at 600°C, the α/(α+β)-transition temperature, type of SPP in the Zr rich corner, and their max existing temperature, are summarized for interesting alloys. The solid solubility reaches significant values only if the atomic misfit is less than 10% (for substitutional soluted elements), as for elements Ti, Nb, Sn, Sb, Ta, and Bi in α-Zr respectively ≥44% (for interstitialy soluted elements), as O, N, and H. Elements O, N, Sn, Ge, Y, and Bi extend the α-range to higher temperatures (α-stabilizer), whereas H, C, V, Cr, Mn, Fe, Ni, Cu, Nb, Mo, Ta, W, and Pt extend the β-range (β-stabilizer). The SPP observed in the Zr rich corner are either Zr_3E,, Zr_2E, Zr_3E_2, ZrE, or ZrE_2 (E for second element) The highest existence temperatures are seen for ZrE type SPP, the lowest for Zr_3Fe and Zr_3Bi.

The binary phase diagrams for the most interesting elements are given the following.

2.2.1 Binary Phase Diagram Zirconium-Oxygen

Oxygen is rather an alloying element than an impurity at least for most of the Zr-alloys. It is added to increase the strength. The normal impurity content is 300 to 700 wt ppm (0.2-0.45at%) in the Zr alloys produced from Zr sponge. Whereas in Russian Zr alloys, produced from a mixture of electrolytic and iodine Zr, oxygen is kept at the impurity level, ZrO2 powder is added during melting for most Zr alloys in USA, France and Japan with the goal to get a definite oxygen content in the range between 1000 and 2000 ppm (0.65-1.3 at%). The Zr-O binary phase diagram is given in Figure 2-1. O has a high solubility. At the operation temperature of water cooled reactor fuel (300-400°C) at concentrations >16 at% (>4 wt%) α2, α3, and α4 phases (Zr_nO phases with n=3.5, 3, and 3.5) can form and at >30 at% (>7 wt%) ZrO_2. α-ZrO_2 is monoclinic and transforms to tetragonal β-ZrO_2 at 1205°C. Oxygen in solid solution stabilizes the α-Zr. An increase of the α/α+β temperature of 10°C per 100 ppm was observed in the range 600-1800 ppm by Miquet, et al., 1982. At >20 at% (>5 wt%) O stabilizes the α-phase of Zr up to the melting point. During high temperature oxidation experiment (>1000°C) a layer of oxygen stabilized α-Zr is formed between the β-quenched structure and the zirconia due to the inward diffusion of oxygen. Slow cooling rates through the α+β range or annealing within the α+β rage can result in O inhomogeneities (enrichment in α, and depletion in β phase)

2.2.2 Binary Phase Diagram Zirconium-Tin

Addition of 0.5 to 1.7 wt % (0.4-1.3 at%) of tin makes the alloy more tolerant towards material impurities (such as nitrogen) and impurities in the water (as LiOH) that otherwise would deteriorate the material corrosion performance. Sn-additions also increases the material strength. Sn is, as oxygen, an α-stabilizer. It has in both the α-Zr and the β-Zr a substantial solid solubility. The Zr-Sn binary phase diagram is shown in Figure 2-2. Additions of >4.9 at% (>6.4 wt%) tin increases the α/β transition temperature to 962°C. The solid solubility at fabrications temperatures of claddings (>600°C) is >2 wt%. However, at operation temperatures of water cooled reactor fuel (300-400°C) the solubility is only a few tenth of a %, Dupin, et al., 1999. At higher Sn contents the tetragonal Zr_4Sn phase should appear according Figure 2-2. However, Zr_4Sn is only weakly stable against the decomposition of Zr_4Sn in α-Zr and the hexagonal Zr_5Sn_3, because rather low levels of Fe impurities make the Zr_4Sn Phase unstable, Tanner and Levinson, 1960. Annealing in the α+ß-range result in an enrichment of Sn in the α phase and a depletion of Sn the ß phase (see also Miquet, et al., 1982).

Table 2-2: Atom number, atom weight, neutron cross section, atom size, atom misfit, solubility at 600°C, α/(α+β)-transition temperature, and type of SPP in the Zr rich corner.

Elem.	Atom number	Atom weight	Therm Cross section, barn	Atomic radius, Å	Atomic misfit, %	Solubility at 600°C, at%	α/α+β trans. Temp., °C	Type of SPP	Max. existing temp., °C
H	1	1.008	0.332	0.78	-51	6	550	Zr_2H	
C	6	12.011	0.0034	0.92	-43	~0.01	800	ZrC	3427
N	7	14.007	1.85	0.88	-45	22	1880	ZrN	3410
O	8	15.999	0.00027	0.89	-44	30	1940	Zr_2O	2710
Si	14	28.08	0.966	1.319	-18	~0.01	863	Zr_3Si	1650
S	16	32.07	0.52	1.27	-21	0.003		Zr_3S_2	
Ti	22	47.88	6.1	1.462	-9	100	863		
V	23	47.88	5.04	1.346	-16	<0.1	777	ZrV_2	1300
Cr	24	50.942	3.1	1.321	-18	0.01	831	$ZrCr_2$	1560
Mn	25	51.996	13.3	1.284	-20	<0.1	790	$ZrMn_2$	(1140)
Fe	26	54.938	2.55	1.274	-21	0.01	795	Zr_3Fe, Zr_2Fe	885 998
Ni	28	58.933	4.43	1.246	-22	0.01	845	Zr_2Ni	1120
Cu	29	63.564	3.79	1.278	-20	<0.1	822	Zr_2Cu	1000
Ge	32	72.61	2.3	1.369	-14.5	~0.1	896	Zr_3Ge	1587
Y	39	88.906	1.28	1.801	12.4	<0.1	880	α-Y	
Zr	40	91.224	0.185	1.602	0		865		
Nb	41	92.906	1.15	1.468	-8.4	0.5	620	β-Nb	
Mo	42	95.94	2.65	1.40	-12.6	<0.1	738	$ZrMo_2$	1880
Sn	50	118.71	0.63	1.584	-1.1	2	980	Zr_4Sn	1327
Sb	51	121.75	5.4	1.59	-0.7	0.5	875	Zr_3Sb	
Te	52	127.6	4.7	1.60	-0.1	~0.1	863	Zr_3Te	1354
Ta	73	180.95	21	1.467	-8.4	0.5	801	β-Ta	
W	74	183.85	18.5	1.408	-12.1	<0.1	833	ZrW_2	2160
Pt	78	195.05	10	1.387	-13.4	<0.1	827	Zr_2Pt	1727
Bi	83	208.98	0.033	1.70	+6.1	3	901	Zr_3Bi Zr_2Bi	901 1342

3 BASICS OF THE CORROSION PROCESS (B. COX)

3.1 GENERAL CONSIDERATIONS

The growth of oxide films (or more generally scales not necessarily of oxide) has been treated extensively in the early literature, Wagner, 1933; Cabrera and Mott, 1949; Hauffe, 1965. If the rate of growth of scale is decreased with increasing scale thickness it is usually concluded that the rate of corrosion is controlled by the diffusion of some species through the scale. Consideration of the chemical composition of the scale being formed, and the thermodynamics of the system will then give an indication of what the common defect concentrations in the scale will be as a function of temperature and the oxidation potential of the environment. All reactions leading to scale growth (with the exception of the formation of hydride layers) are oxidation reactions. The difference in the thermodynamic conditions at the outer and inner interfaces of an oxide scale will lead to a concentration gradient in the primary defects in the scale. Most of this early work was related to metals forming electrically conducting scales, so the possibility of an electric field developing across the scale was ignored. The primary defects whose concentration gradients determined the rate of corrosion were then either anion or cation vacancies (or both) in the scale.

In the case of the growth of oxide films the concentration gradients of the defects can be calculated for each of the oxide interfaces (oxide/environment and oxide/metal respectively) from oxygen partial pressures calculated for each interface. The rate of diffusion of each type of defect through the oxide film can then be calculated from their concentrations and measurements of the diffusion coefficient of each of the possible species (c_1, c_2…c_i). Although these diffusion coefficients can be calculated theoretically if the geometry of the defect is well enough known to allow the difference in free energy between its equilibrium and saddle-point energies to be calculated, in practice they must be measured.

From the measured diffusion coefficients the fluxes of particular defects can be calculated using Fick's 1st Law. The restrictions assumed for the derivation of the oxidation rate have usually been that there be no electric field across the oxide and no local space charge. Given these boundary conditions then the above diffusion processes of lattice defects would be the only processes for transporting material through the oxide. The assumption is also made that the partial oxidation processes creating ionic and cationic defects occur at one or other of the two oxide interfaces. This has been somewhat contentious because of some arguments that in some oxidation systems, where both anions and cations are completely mobile, recombination of these defects to form fresh unit cells of oxide within the bulk of the oxide could occur. However the actual mobile species is the anionic or cationic vacancy which progresses right through the oxide, while the individual anions and cations only hop one lattice spacing at a time, and preserve their order in the oxide (apart from some lattice mixing). Where both anions and cations are mobile the fluxes of both must be summed, and the total fluxes can be converted into thicknesses of oxide formed in unit time if the partial specific volumes of each mobile species are known. These partial specific volumes can be calculated from a detailed knowledge of the crystallography of the oxide being formed. Integration of these fluxes gives the well known parabolic growth law first observed experimentally by Tamman, 1920.

$$l_i^2 - l_o^2 = 2Kt \qquad \text{Eq (1)}$$

where l_0 and l_i are the initial and final oxide thicknesses

t is the time, and

k is the parabolic rate constant

The boundary conditions required for the application of the Wagner-Hauffe Theory of oxidation are quite restrictive:-

(i) Both the metal and the oxide should be homogeneous in the plane of the oxidising surface. Ideally both should be monocrystalline, or if not there should be no evidence for preferential diffusion at grain boundaries. If there is such preferential diffusion then the "effective diffusion coefficient" needs to be known. In practice most measurements of diffusion coefficients in a polycrystalline oxide will give the "effective diffusion coefficient".

(ii) Only diffusional transport should be rate-determining. In the presence of electric fields the transport process will obey different laws.

(iii) Ionic and electronic motions must be coupled to maintain local electroneutrality.

(iv) Cationic and anionic transport should be of comparable difficulty.

These limitation to the Wagner-Hauffe Theory's applicability are least arduous for the growth of thick electrically conducting oxides at high temperatures. Under such conditions the effects of localised diffusion at grain boundaries, and of any space-charge layers at the oxide interfaces will be minimised. For thin oxide films formed at relatively low temperatures where space-charge layers are likely to modify the diffusion process, Fromhold, 1976, has developed oxide growth laws which are closer to inverse logarithmic than parabolic. These are achieved by dispensing with the requirement for maintaining complete local electroneutrality and allowing coupled currents, where the net current through the oxide is zero. This approach can result in large internal electric fields in the oxide and inhomogeneous space-charge distributions.

In the presence of an electric field across the oxide the total flux of the charged species will be given by the sum at the fluxes due to diffusion and "electrolysis" (migration under the influence of the electric field). The simplest case to consider is one where there is a constant voltage applied across the oxide and the electric field decreases as the oxide thickens (this is in essence a high temperature anodisation process). An approximate expression for such a situation can be derived, Fromhold, 1976; TECDOC – 996, 1998.

In practice such experiments are difficult to perform because of the problems inherent in providing a reversible electrode contact on the outside of the oxide that will provide the constant voltage across the oxide, but will not impede the diffusion process at this surface. The nearest approach to this may be the oxidation experiments performed in oxidising fused salts, Wanklyn, 1958; Cox, 1969. Similar experiments in high temperature aqueous electrolytes are limited by the poor reversibility of most external electrodes for electronic currents, Urquhart, et al., 1978. Experiments that attempt to maintain a constant current through the oxide are not recommended because of the possibility that local current carrying paths in the oxide would carry excessively high fractions of this current leading to local ohmic heating and damage to the oxide. Such locally high current densities may of course occur under constant voltage conditions, but can more easily be controlled.

3.2 APPLICABILITY TO ZIRCONIUM ALLOY OXIDATION

Oxide films on zirconium alloys have very different properties from those envisaged by the Wagner-Hauffe Theory, and therefore require some modifications in the interpretation of the data. These differences can be enumerated:-

a) Thermodynamically zirconium dioxide is one of the most stable oxides, but oxygen in dilute solution in the metal phase is even more stable. Thus, there is always an equilibrium between oxide formation and oxygen dissolution in the metal, Figure 3-1.

4 MAJOR FACTORS AFFECTING CORROSION

4.1 EFFECT OF TEMPERATURE (A. STRASSER)

4.1.1 Introduction

Temperature is one of the most important parameters affecting zirconium alloy cladding corrosion. Yet it is a parameter that can not be measured directly --- it can only be calculated. Uncertainties in the calculations, or modeling, are the results of uncertainties contributed by numerous other parameters that are necessary components of the models, some of which are equally difficult to measure. *Knowledge of the parameters that affect the temperature and an appreciation of the uncertainties related to each parameter are important in the evaluation of the relationship of temperature to in-reactor corrosion.*

Temperature measurements of samples in ex-reactor tests or some test-reactor tests (particularly of unfueled samples) can be made reasonably reliably. *The objective of this section is to identify the various parameters that affect the temperature of cladding during in-reactor service, note their degree of importance and provide the reader with some feeling of the uncertainties involved.*

Ex-reactor corrosion tests of zirconium alloys with initially clean surfaces provide the data that show the dramatic increase of corrosion with temperature. An example from work by Bettis Labs. is shown on Figure 4-1, a 26% increase in weight gain due to a 5°C increase for a nearly 7 year long test at a typical cladding temperature of 335°C. The “typical” maximum cladding temperatures are summarized in Table 4-1 for BWRs and PWRs along with the reactor inlet and outlet coolant temperature ranges. The cladding temperatures are calculated numbers for clean surface cladding at nominal reactor operating conditions.

Table 4-1: LWR Coolant and Cladding Temperatures, Nuclear Engineering International, 1998.

	BWR	**PWR**	**VVER-440**
Coolant Inlet Range			
^{o}C	272-278	279-290	267
^{o}F	522-532	534-554	513
Coolant Outlet Range			
^{o}C	280-300	313-330	296-300
^{o}F	536-572	595-626	565-572
Max. Clad Temperature			
^{o}C	310-320	318-360	335-345
^{o}F	590-608	604-680	635-653

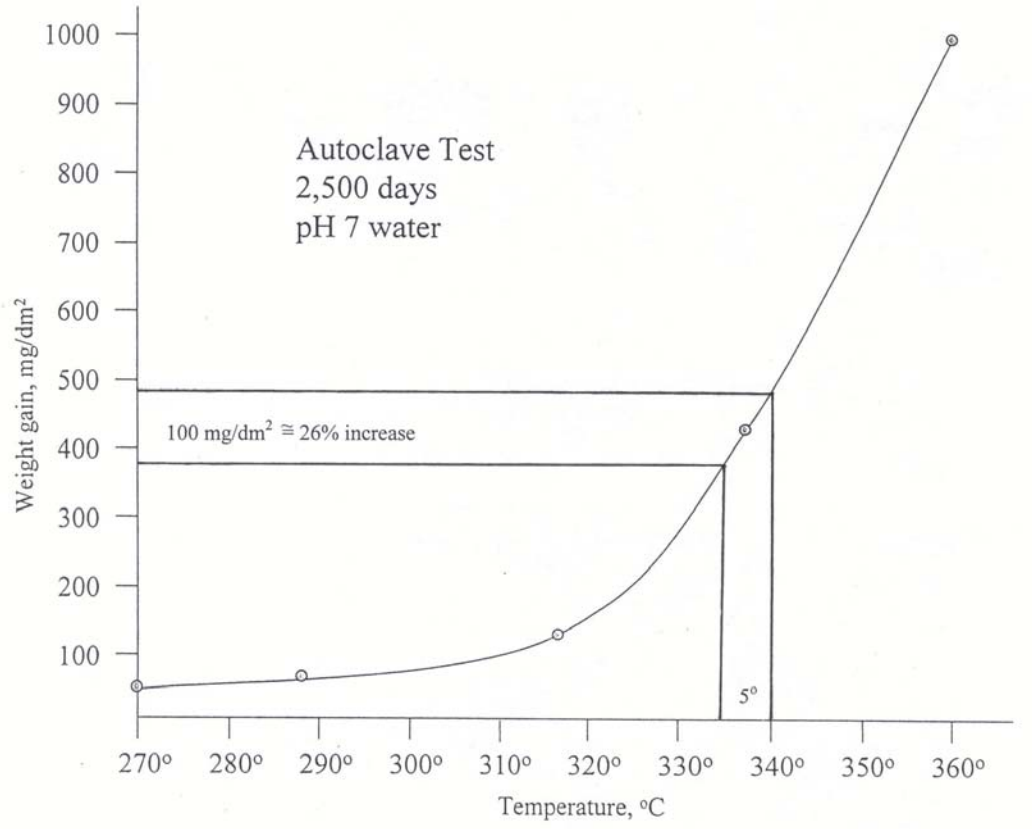

Figure 4-1: Zircaloy 2 and 4 weight gain as a function of temperature, Hillner, et al., 2000.

The lower pressure and the boiling regime of BWRs limit their coolant temperatures and inlet to outlet temperature ranges compared to PWRs. Greater flexibility in PWRs also permitted them to increase coolant outlet temperatures (and peak cladding temperatures as a result) for the more modern units in their race to increase efficiency and lower the predicted fuel cycle costs. It is interesting to note that due to the high corrosion rate of cladding at the high temperatures many of these newer PWRs have modified their system to reduce temperatures and lengthen the life of their fuel cladding.

The Russian VVER 1000 units fall within the temperature range of the western PWRs, but the VVER 440 units are lower in temperature and are shown separately for that reason.

A brief overview of the relationship of PWR coolant temperatures and cladding corrosion is given in Table 4-2. At an exposure of 45-48 GWD/T the oxide thickness on Zircaloy-4 claddings range 11-37 μm in the lowest coolant temperature early PWR (Ginna) to 78-120μm in one of the more recent, high temperature plants (Gösgen), by a factor of about 4. The other plants cited are in a range of coolant temperatures and oxidation levels between these two extremes.

Table 4-2: Corrosion of Standard Zircaloy-4 as a Function of Plant Parameters, IAEA, 1998.

Plant	Ave. Core kw/lit.	Ave. Core Outlet °C (°F)	Oxide Thickness, μ	Burnup-GWD/MTU	
				Rod	Assy
Ginna	89	317 (602)	11-37	45-48	42.5
			20-41	54-56	52
ANO-2	97	323 (613)		58 (ave.)	52
			21-73	57-60	
			40-80	60-64	
Grohnde	95	327 (602)	82-92	45-46	
Summer	105	327 (620)	76-86	46-48	46
North Anna	109	327 (620)	52-96	44-47	46.4
Gösgen	101	325 (618)	78-120	40-48	

The temperature at the interface between the zirconium alloy metal surface and the zirconium oxide formed in the corrosion process is the most critical in determining the corrosion rate. The variables that determine this temperature are shown pictorially in Figure 4-2 and are listed in Table 4-3. As shown on the Figure, the interface temperature in question is determined by the power or heat flux (Q) generated in the fuel rod and the efficiency of the coolant in removing this heat. The thermal resistance of the oxide and the crud layers between the coolant and the metal surface need to be taken into account in the calculation of the metal oxide interface temperature.

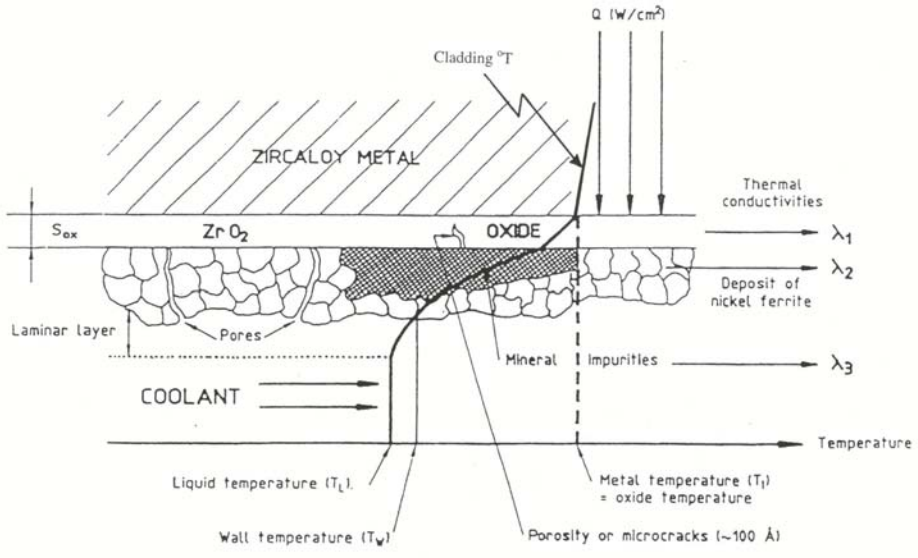

Figure 4-2: Factors that affect cladding temperature, IAEA, 1998.

5 CORROSION MODELING (P. RUDLING)

5.1 INTRODUCTION

5.1.1 Design limits on oxide thickness

Appropriate performance of the zirconium alloy materials is crucial to maintain trouble free reactor operation. *General Design Criteria 10, GDC 10,* in the document *Title 10-Chapter 1, Code of Federal Regulation Part 50* of *Nuclear Regulatory Commission, NRC,* specifies that the fuel assembly including the fuel rod may not be *damaged* during class I and II operation. With the wording *not damaged*, means that the fuel rods may not fail, that fuel rod and assembly dimensions remain within operational tolerances, and that functional capabilities are not reduced below those assumed in the safety analysis. Chapter 4.2 in *Standard Review Plan, SRP*, interprets *GDC 10* and identifies certain criteria, named *Specified Acceptable Fuel Design Limits, SAFDL*s, that the fuel design must meet. The intent of the *SAFDL*s is that if the fuel design meets these criteria, *fuel damage* will not occur during class I[10] and II[11] operation. Each *SAFDL* is related to a specific fuel damaging mechanisms and the design and operational margin towards each *SAFDL*s is intimately related to the fuel rod power operation. The margin towards *fuel damage* is constituted by the operational/design and safety margins, Fig.5-1. In general lowering rod power reduces the risk that the fuel will become *damaged* during irradiation, Fig. 5-1.

[10] Normal operation including some frequently occurring transients
[11] Anticipated operational occurrences – power transients with an occurrence of about 1 per reactor year.

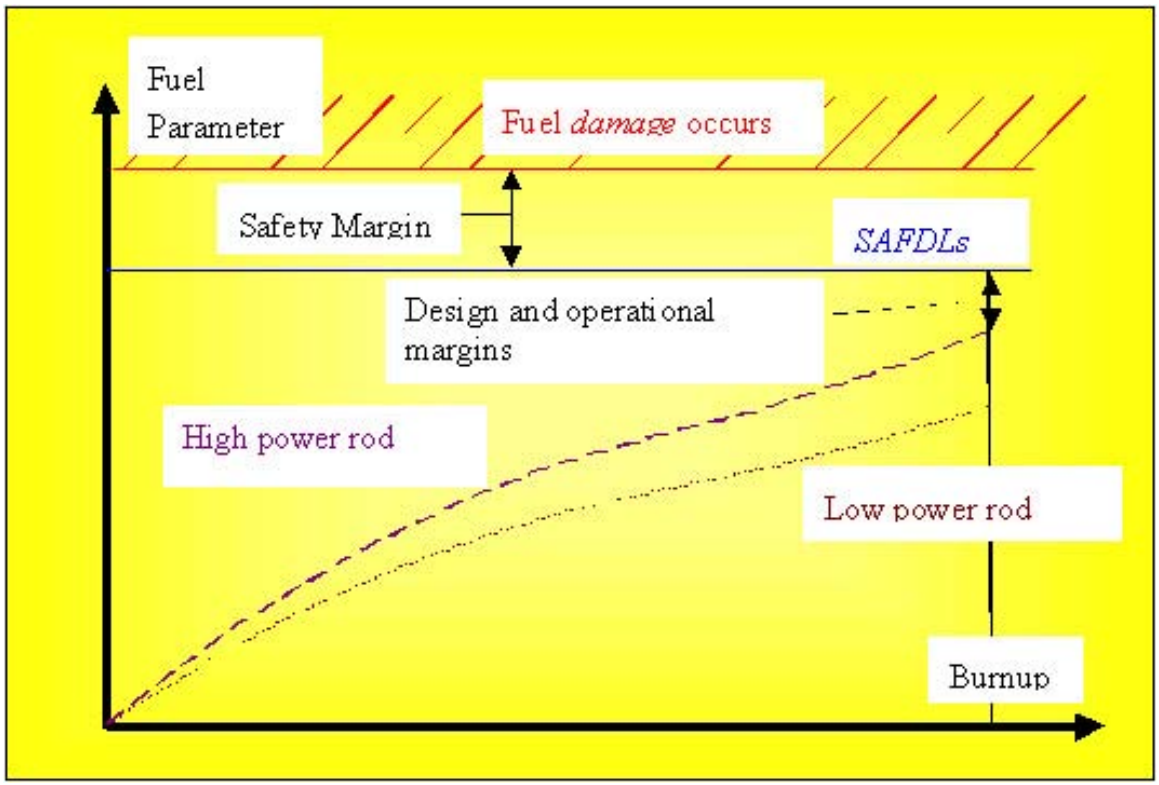

Figure 5-1: Schematics showing the design and operational margin that exists between any "fuel parameter value, e.g. oxide thickness value" and its corresponding *SAFDL*, e.g. 100 μm. This figure also shows that there normally exists a Safety Margin between the SAFDL value and the value at which fuel is damaged (in the case of oxide thickness). If the oxide thickness value exceeds the safety margin, the fuel rod fails due to through-wall oxidation.

In the SRP, section 4.2, the *SAFDL* related to maximum allowable oxide thickness and hydrogen content in any Zircaloy fuel component in the fuel assembly (fuel rod, grid, fuel outer channel,…) states the following:

Oxidation, hydriding and CRUD deposition should be limited. The maximum allowable oxide thickness, hydrogen content and CRUD deposition should be discussed (by the fuel vendor) *and the proposed limits* (by the fuel vendor) *should be verified to be acceptable in the Safety Analysis Report. The stress and strain calculations should be based upon assuming the maximum allowable oxide thickness, hydrogen content and CRUD deposition on the fuel components. The effect of CRUD deposition should also be taken into account while calculating the thermo-hydralic performance of the fuel (that is more discussed in SRP section 4.4).*

The reason for maximising the allowable oxide thickness for non-heat-transfer components, such as e.g. grids and fuel outer channels, is that the oxide mechanical strength is much lower than that of the zirconium alloy material and oxidation will consequently reduce the load-bearing transversal cross-section area, thus increasing the stress of the component subjected to the load.

On the other hand, the original rationale for specifying a maximum oxide (and CRUD) thickness for fuel claddings is related to that an increase of temperature lowers the cladding mechanical strength. If the oxide and CRUD layer thickness become too large, the resistance towards the heat flux will become significant and a further increase in the thickness will raise the cladding temperature further. This raise in temperature will increase the cladding corrosion rate thus increasing the oxide thickness further resulting in an even higher cladding temperature. Consequently, a thermal feedback effect may be the result that could increase the cladding temperature and thereby lower the material strength to such an extent that the cladding may mechanically fail due to a postulated clad tensile stress. However, in reality, mechanical failure of the fuel cladding does not occur due to that the stresses are too small. Instead, the thermal feedback effect will cause corrosion acceleration resulting in fuel clad failure by through wall oxidation, see e.g. section 6.1.

The maximum oxide thickness criterion used today by *NRC* for PWR applications is 100 μm. *NRC* has specified that this maximum oxide thickness is the average value along the cladding circumference in a transversal cross section, which means that much higher values, may exist locally without exceeding the criterion. There are no corresponding *NRC* limit for BWR applications, the reason being that the temperature dependence of corrosion rate is much smaller in BWRs than in PWRs, see section 4.1. Somewhat different design limits on oxide thickness are used by regulatory bodies in different countries but these limits are close to 100 μm.

To ensure that the Zircaloy material will not become so brittle that it will fail if stressed, the hydride concentration (as a result from in-pile corrosion) in the material must be limited. *NRC* has however not given a specific maximum allowable hydrogen content in the Zircaloy material. Most fuel vendors were using a maximum hydrogen content of 500-600 wtppm but are now trying to get away from this limit primarily since they may have difficulties containing the hydrogen content below this limit for high burnup fuel. *It is however noteworthy that this limit was most likely assessed by room temperature, RT, mechanical tests of hydrided Zircaloy and at 500-600 wtppm of hydrogen the material may become brittle at RT. It is questionable if this test temperature is relevant since, during operation condition the hydrided material becomes much more ductile (due to higher temperature) and much higher hydrogen concentrations can be accepted in the material without getting a brittle behaviour.* There is no consensus in the industry on how the hydrogen content in the component should be assessed, e.g., one fuel vendor calculates the hydrogen content as the average value in the whole component while others may take the average value in the fuel clad cross section. *The material response is however not only dependant upon the hydrogen concentration but*

6 CORROSION FAILURE MECHANISMS AND EXAMPLES

6.1 CORROSION FAILURES IN PWRS (G. WIKMARK)

Accelerated uniform corrosion in PWR plants can be obtained from thermal overheating (see Section 4.1), a water chemistry impact (see Section 4.3) or an acceleration from high hydrogen contents in the cladding (see Section 4.4.3).

Thermal overheating could be obtained from departure from nucleate boiling, dnb, a situation when the water film on the cladding surface is not fully covering and the cladding will be (locally) overheating. This effect is given by the fuel design, core design, and the operation, and should be limiting in the fuel design and operation to avoid dnb situations.

Thermal overheating could also result from crud deposits, forming a thick and thermally insulating layer, see Sections 4.1 and 4.3. Several cases of this kind leading to fuel failures have been experienced the last years, as described in Section 6.1.1.

It is also known that more oxidising conditions may produce nodular corrosion in PWRs, see Section 4.3, but fuel failures have not been reported from such a situation.

6.1.1 Crud Induced Fuel Failures

Fuel failures were observed during cycle 10 in Three Mile Island, TMI, coupled with crud formation, revealed in the form of "distinctive crud pattern" (DCP), i.e. circumferentially uneven crud deposits, recorded after shutdown[24], Mitchell, 1997; Mitchell and Thomazet, 1998. The boron concentration had been extremely high at the beginning of cycle (BOC) 10, starting at 1851 ppm. A maximum of 2.2 ppm lithium was used and hence the pH at BOC of cycle 10 was considerably lower than 6.9. Fuel failures were indicated by radiochemistry spikes after 122 days of operation. Some axial offset anomaly, Wikmark and Cox, 2001, AOA[25], effect was found reaching a maximum in the middle of cycle 10.

109 degraded fuel pins were found at EOC 10, whereof 9 had failed by through-wall defects. The degraded fuel pins had 2 – 70% cladding wall thinning from the outside diameter due to corrosion, concentrated to the 2.8 m axial level, Mitchell, 1997. The cladding oxide thickness of the rods with the DCP s was less, although the crud layers were significantly thicker on these rods up to 33 µm thick. The specific activity of the DCP crud was higher, indication of a more tenacious crud.

[24] The crud found after shut-down in a PWR is normally much less and possibly in different form than at operation. The reason for this is the more acidic and eventually oxidising chemistry applied during the shut-down in order to strip the crud deposits from the fuel cladding. Any records of fuel crud obtained after such a shut-down procedure might at best provide partial information about the real situation during operation.

[25] A situation when crud deposit in the upper part of the core enables co-precipitation of boron in the crud, leading to a power suppression in that region. Subsequent power reductions often seem to allow redissolution of the boron, and since the boron is normally not redeposited by return to the former power level, now instead a local power increase is found in the previously power suppressed region, due to a lower local burn-up and plutonium enrichment. The AOA phenomenon seems to correlate to high nickel levels in the corrosion products depositing on the fuel cladding and subcooled boiling on the highest-duty rods, which are the rods affected by AOA.

All failed and degraded pins had DCP. Calculations indicated that no boiling should have occurred on the pins with DCP, although the pins with DCP were calculated to have a slightly higher temperature. Nevertheless, the cladding temperatures[26] in the DCP areas were calculated to have been extremely high. The calculations further showed that once the crud layer was 10 – 20 µm thick, boiling on the cladding surfaces could be expected. Most crud was found on the peripheral sides of the rods. No signs for a temperature difference around the circumference for the affected rods could, however, be found.

AOA and subsequent fuel failures occurring during the same cycle were reported from Palo Verde-2 in 2001, Govertsen, 2001; ZIRAT-6 Report, Section 7, 2001, very similar to the previous incidence in TMI, see Figure 6-1.

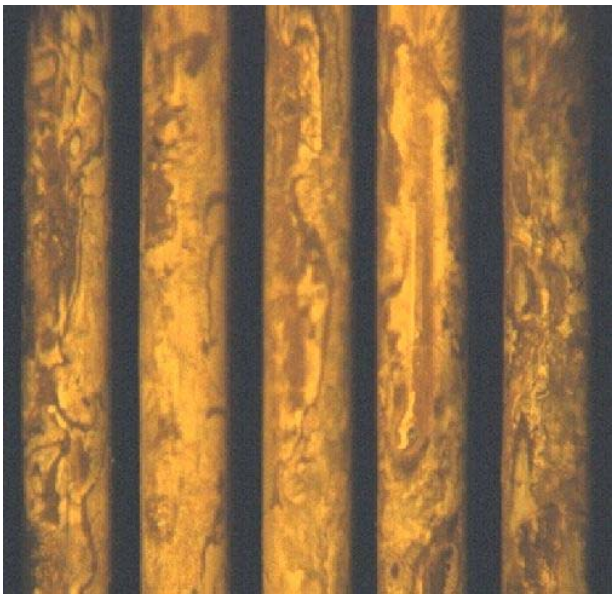

Figure 6-1: Cladding with accelerated corrosion from Palo Verde in 2001, Govertsen, 2001. Some of the rods hade through-wall corrosion.

One of the suspected important factors was a cold shutdown early in cycle 9 (which began in early May 1999). It is speculated that the cold shutdown did release substantial amounts of crud, redistributed from older fuel to the fresh fuel, operating at higher duty. Indications of AOA were recorded soon after the start-up after the short cold shutdown. Another mid-cycle cold shutdown removed the AOA indications but soon after the start-up fission gas releases suggested many large fuel failures, Govertsen, 2001. Tenacious crud was found at a post-cycle inspection, but only slightly thicker (still < 50 µm) than previously recorded for Palo Verde Units 2 and 3.

[26] That means the temperature in the metal oxide interface, where the corrosion takes place.

The proposed cause of the failures in Palo Verde 2 was “loss of AOA” leading to enhanced local power in some rods. It is believed that the same mechanism was also experienced in TMI (in 1995). *It has been indicated that also some fuel failures in Seabrook, from which no details have been published since the incident in 1998 were caused by a similar mechanism.*

The number of plants having AOA and subsequently developing fuel failures has hence possibly been some 10% for the 30 AOA affected cycles during the last 10 years, ZIRAT-6 Report, Section 7, 2001.

6.2 CRUD RELATED FAILURES IN BWRS (A. STRASSER)

6.2.1 Introduction

The major sources of crud formation on the fuel rod surfaces in BWRs (as in PWRs) are the metallic impurities in the coolant, that result from the corrosion of the reactor coolant system materials. Other sources are the in-leakage of solids, liquids and gases into the system and impurities from the surface of components placed in the core (fuel assemblies, etc.). A schematic of the coolant system corrosion, corrosion product transport and deposition process is shown on Figure 6-2.

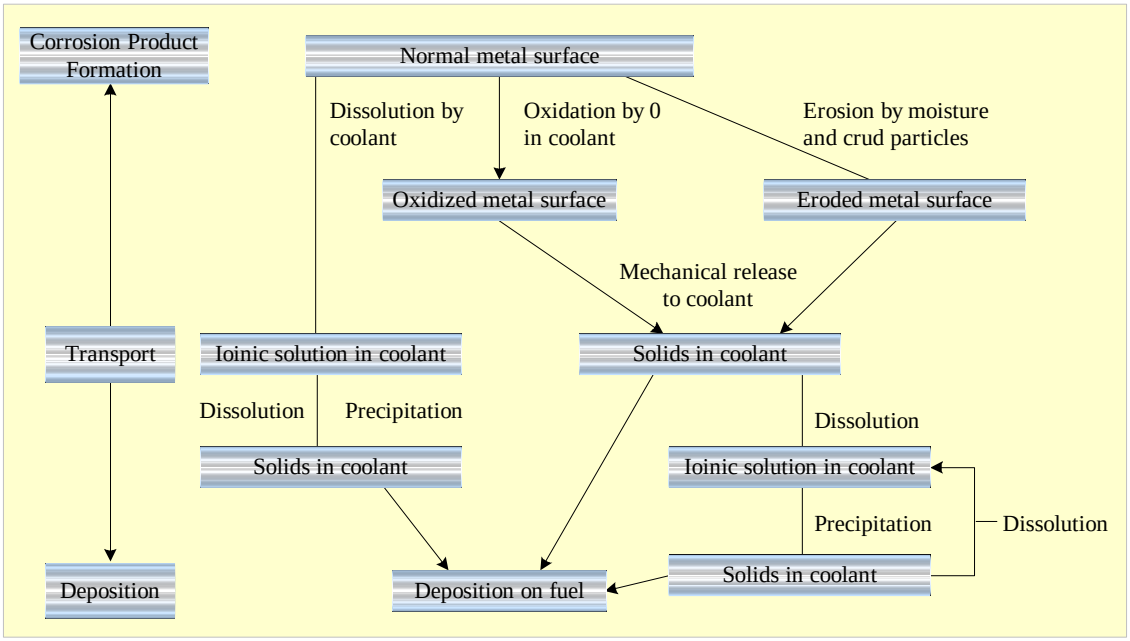

Figure 6-2: Sources of Corrosion Deposits (crud) on Fuel, Strasser, et al., 1985.

Iron oxide is the major source of crud in the form of Fe_2O_3 with traces of Fe_3O_4 and iron hydroxides.Minor amounts of Ni, Cr, and Co are also present. The major source of iron is the corrosion of carbon steel components. The second most significant constituents are Cu and Zn from the brass condenser or Zn injected to reduce activity transport (GEZIP process).

7 GRAND COMPARISON OF CURRENT ALLOY EXPERIENCE (P. RUDLING)

To compare the corrosion performance of various zirconium base alloys one has to consider the following:

- For corrosion performance of an arbitrary material, the oxide protectiveness is crucial, that is a function of the metal microstructure and the environment. However, the environment for the zirconium materials in-pile are changing, new water chemistry regimes and operation strategies are implemented. Thus, a relevant comparison of performance must not only include current environment but also projected environments in the future must be considered. It may be that a certain ranking between materials exists during current corrosion environments but that the ranking will change considering future corrosion environments. The following trends may have a significant impact on zirconium material performance:
  - Increasing burnup
  - Implementing new water chemistry regimes such as:
    - Increased LiOH and Zn-injection in PWRs
    - NMCA, Zn-injection in BWRs
  - More aggressive loading schemes in PWRs resulting in more subcooled boiling that in turn will increase LiOH concentration in the zirconium oxide.
- Not only the average corrosion performance of an arbitrary zirconium material is important but also its scatter in corrosion behaviour. This scatter depends on:

- The robustness of the zirconium material that is a function of its microstructure. A zirconium material that is less robust considering corrosion performance shows more scatter in corrosion data since the environment of such a material have larger impact. On the other hand, a material that has a robust microstructure will have a corrosion performance that is less sensitive to the environment (water chemistry and loading schemes). This situation is particularly important for the current material development for PWRs, where new materials such as M5, ZIRLO and DUPLEX-ELS may show superior corrosion performance during normal water chemistry conditions compared to that of Zry-4. However, it is not clear that the same ranking will exist during off-normal conditions, e.g., during air-inleakage or some other water off-normal water chemistry transient. Since these types of conditions rarely occurs one has to wait for a long time before we have enough data to make a relevant comparison between different alloys. It is important to consider that the amount of data on Zry-2 and –4 has been collected for more than 30 years, while very little data exists for promising new alloys.

  For a true robust material, the zirconium metal microstructure must remain unaffected by the environment. Thus, such a robust material should show a microstructure that is not impacted by the fast neutron flux. This is e.g. not the case for current BWR materials where the second phase particles are slowly dissolved into the zirconium matrix.

- Zirconium material sensitivity towards manufacturing variations. No manufacturing process is perfect and there will always be small differences during manufacturing such that different materials will experience a difference in e.g. temperature cycle in the heat treatment furnace, etc. For a robust material, significant variations in manufacturing processes should not significantly change the zirconium microstructure in the final product. New alloys are normally manufactured during very stringent manufacturing conditions and the situation will be very different during subsequent manufacturing of the material when it becomes a commercial product. The robustness of a material relative to manufacturing process variation may only be assessed when a large quantity of the material, e.g., cladding tubes have been manufactured over time. Thus, when comparing corrosion data it is important to consider how many different material lots[27] constitutes that data set.

In the following sections a comparison of various commercial and experimental alloys as tubes and sheets are provided. **It is however, very important to keep in mind that a true comparision is very difficult since the different fuel vendors choose to present their data in different ways. Siemens BWR oxide thickness data are the peak oxide thickness value per rod while other fuel vendors provide some rod average oxide thickness value. In many cases it is also not clear from the data how the data has been generated (is it rod maximum value or some rod average value).**

[27] A material lot is defined as the same set of materials, e.g., cladding tubes that has been heat-treated at the same time. Heat treatments during manufacturing is normally done in batches.

Also, fuel vendors normally do not provide all oxide thickness data, e.g., cases with very high oxide thickness values are normally not reported. For PWRs normally, all fuel vendors are providing the are provide the rod maximum oxide thickness but again a true comparison is difficult since the data are generated in different plants with different power histories and water chemistry largely impacting corrosion performance.

7.1 BWR MATERIALS

7.1.1 Commercial materials

7.1.1.1 Uniform corrosion of BWR sheet materials

Some limited corrosion data from fuel channels as well as spacer grid materials are presented in Figure 7-1. Since it is not known what type of sheet materials, Zry-2 and/or Zry-4 constituted the Siemens data no comparison can be made between Siemens and Westinghouse-Atom data. Also in the Westinghouse-Atom case no differentiation has been made between uniform and shadow corrosion data.

It appears however that corrosion performance is significantly better for Zry-2 compared to that of Zry-4-which is no surprise. The existence of Ni in Zry-2 (that is missing in Zry-4) has a dramatic effect on lowering the corrosion rate, however, adding Ni also increases hydrogen pickup fraction[28].

[28] Hydrogen pickup fraction is the fraction of hydrogen, released by the corrosion reaction between water and Zircaloy, that is pickup up by the Zircaloy material. The total amount of hydrogen pickup e.g. in ppm, is the product of hydrogen pickup fraction and the corrosion rate (that determines the amount of hydrogen produced).

8 SUMMARY

The intent of this special topical report is to provide members with all important aspects related to LWR corrosion performance to allow the utility to implement actions to reduce corrosion. The report covers the range from basic information to current knowledge.

The corrosion environment is quite different in pressurized water (closed cycle) reactors and boiling water (open cycle) reactors. In the PWRs the environment can be optimized by additions (hydrogen, boric acid, lithium hydroxide) whereas in the BWRs the environment within the core can be only very little influenced and is highly oxidative. The input of products from the corrosion of the structural surfaces can vary significantly and depends widely on the materials and the water chemistry applied. As consequence, the quantity of deposits on fuel rods can differ.

Zr alloys for fuel claddings were developed at first in the 50ies (Zircaloy-2 and -4 in USA, and E110 in Russia). Zr alloys experience in water and steam different types of corrosion, as uniform corrosion, nodular corrosion, shadow corrosion, and several kinds of late accelerated corrosion (e.g by hydrogen, precipitate dissolution etc.). Optimization of the cladding materials developed in the 50ies for increased burnup and robustness started in the 80ies and is still ongoing. Today, an optimized Zry-2 is used for BWR fuel elements whereas for PWR fuel assemblies besides optimized Zicaloy-4 several new Zr alloys (as ZIRLO, DUPLEX-ELS, Modified Zircaloy-4, M5) are applied for reloads.

The corrosion behavior of Zr alloys depends on alloying content the solute content and the intermetallic precipitates (SPP). Thus for the most interesting alloying elements the phase diagrams (the solid solubility and the types of SPP) are given in this report. In α-Zr O, Sn, and Nb have a noticeable solubility (0.5-30 at%), whereas Fe, Cr, Ni, and Si are almost totally precipitated in SPP (solubility $\leq$100 ppm).

The alloying elements in zirconium alloys (Fe, Cr, Ni, O, C, Si, Nb, V, …) strongly affect corrosion behavior. Amounts of the elements and distribution of the elements as affected by heat treatments are crucial. This is an area where development is still occurring.

The distribution and size of the SPP, one of the most important parameters for the corrosion behavior, depends on the cladding fabrication process. The fabrication steps of importance for corrosion are discussed in this report. The β-quenching step, the process temperatures and times (which can be assessed by annealing parameters), as well as the final cold work and annealing treatment are the most important fabrication steps.

Heat treatment is the primary method to control the microstructure and microchemistry of zirconium alloys. Such control is key to corrosion resistance in those alloys. Even after nearly 50 years of development, heat treatments of Zircaloy are still being refined. To meet the needs of modern BWR and PWR fuel duties, heat treatments specific to each reactor type are currently being used .For the newer PWR alloys, most of which contain Nb to some extent, heat treatment is particularly crucial to ally corrosion and mechanical performance.

New hypotheses for both protective oxide film growth and breakdown must be developed since the zirconium/zirconia system is very different from those systems for which the Wagner-Hauffe mechanism of oxide growth was derived. The principal peculiarities of the zirconium/zirconia system that must be addressed are the following

- only the oxygen is mobile in the oxide film.
- the oxide film is a good electrical insulator, so that conduction of electrons (the other mobile species needed to maintain electrical neutrality) is the rate limiting step in the growth of protective oxide films.

In-reactor the radiation field increases the oxide conductivity, and relaxes the out-reactor limitations on protective oxide growth. As the protective oxide thickens the multiplicity of oxide orientations nucleated at the oxide/metal interface is decreased as some orientations grow preferientially. This leads to an array of columnar oxide crystallites with a crystallographic fibre texture. The columnar crystallites are always normal to the metal surface, irrespective of the metal grain orientation.

At about 2-3microns thickness the protective oxide breaks down. The causes of the breakdown of these protective oxide films are still not well understood. Initially there can be many cycles of breakdown and partial repair. Amongst other hypotheses are:

- Cracking due to differential stresses developing across the oxide.
- Shear due to the transformation of t- to m-zirconia as stresses relax.
- Local dissolution of oxide crystallite boundaries by chemical species in the water.
- Dissolution of small crystals of Sn,Fe, Cr or Si oxides at zirconia crystal boundaries.

Nodular corrosion which was prevalent in BWRs and can only be simulated in the laboratory in high temperature/high pressure steam requires different hypotheses. The close relationship between "nodular" and "shadow" corrosion suggeste that similar causative processes are operating (i.e. galvanic potential differences and enhanced electronic conductivity in the oxide). Nodular corrosion would then be a micro-version of shadow corrosion, with the SPPs providing the cathodes, and the surrounding Zr matrix the anode. The necessity for a large enough cathodic area to provide a significant corrosion current would then explain the dependence on SPP size and number.

Hydrogen uptake arises from the hydrogen released by the cathodic half-cell corrosion reaction, and not from dissolved hydrogen in the primary coolant. At present there are at least three contending hypotheses to explain the uptake mechanism :

- Hydrogen atoms diffuse through the barrier oxide layer at the oxide/metal interface, or through a "window" in it provided by an SPP particle.

- There is no perfect barrier film and the hydrogen enters at flaws that reach the interface. The competing recombination and escape of hydrogen molecules determines the percentage uptake.

- There is sufficient disorder disorder at crystallite boundaries for OH groups to be present.Hydrogen enters by proton hopping between these OH groups.

There is insufficient evidence at present to permit a clear distinction to be made.

At hydrogen concentrations above the solubility limit at operation temperature, hydrides will precipitate. The amount and distribution of hydrides within the zirconium matrix of a reactor component can affect overall corrosion. It is now generally believed that very dense hydrides (50 – 100% of theoretical density) at the corroding surface can markedly increase local corrosion.

Temperature is one of the most important parameters affecting Zr alloy corrosion --- yet it can not be measured in-reactor and must be calculated. Awareness of the uncertainties in the input data to the calculations is necessary for the proper evaluation of the results.

The temperature at the interface of the Zr metal surface and the Zr oxide has a major effect on the corrosion process and is determined by the following variables:

- Heat flux and heat flux history,

- ZrO_2 film properties

- Crud deposit properties

- Laminar boundary layer coolant properties

- Bulk coolant temperature,

Crud deposits can be benign, or sufficiently thick or dense to contain steam blanketing that can raise the cladding temperature to its failure level. In PWRs this has occurred due to low pH operation, excess oxygen levels or ingress of impurities. In BWRs this has occurred due to Cu deposition in the crud, excessive iron oxide type deposits and ingress of impurities.

Nucleate boiling does not raise the cladding temperature significantly, but does promote impurity concentration and corrosion by these impurities.

Hydraulic effects, especially turbulence at spacers, can improve heat transfer and reduce local clad temperature.

9 REFERENCES

Adamson R. B., Cheng B., Kruger R. M., Mack R. J. and Bartosik D. C., "Effects of Heat Treatment on Properties of Zircaloy", Abstract: Zirconium in the Nuclear Industry, 9th Int'l Symposium, Kobe, Japan, 1990.

Adamson R. B., Lutz D. R., Davies J. H., "Hot cell Observations of Shadow Corrosion Phenomena", Proceedings Fachtagung der KTG-Fachgruppe, Brennelemente und Kernbautelle", 29 Februar/1 Marz 2000, Forschungszentrum Karlsruhe, 2000.

Amaev A. D., et al., "Corrosion "of Zr alloys in boiling water under irradiation", 4th Geneva conference, A/CONF49/P/428, 1971.

Ambartsumyan R. S., et al., "Mechanical properties and corrosion resistance of Zr and its alloys at high temperatures", Proc. 2nd Geneva Conf., P/2044, pp. 12-33, 1958.

Andersson B., "The Enhanced Spacer Shadow Corrosion Phenomenon", Fachtagung der KTG-Fachgruppe "Brennelemente und Kernbauteile", 29 February/1 March 2000, Forschungszentrum Karlsruhe, 2000.

Andersson B., Limback M., Wikmark G., Hauso E., Johnsen T., Ballinger R. G. and Nystrand A-C., "Test Reactor Studies of the Shadow Corrosion Phenomenon", Zirconium in the Nuclear Industry: 13th Int'l Symposium, ASTM STP 1423, Moan G. D. and Rudling P., Eds., ASTM, 2002 (in press).

Andersson P-O., "Results from Operation at Elevated pH in PWR Primary Coolant at Ringhals Unit 2, 3, and 4", Proc. JAIF Int. Conf. Water. Chem. Nucl. Power Plants, April 19-22, 1988, Tokyo, Vol. 1, 158- 161, 1988.

Andersson T., et al., "Influence of thermal processing and microstructure on the corrosion behaviour of Zircaloy-4 tubing", IAEA SM 288/59, IAEA, Vienna, 1986.

Asher R. C. and Cox B., "The Effects of Irradiation on the Oxidation of Zirconium Alloys", Proc. IAEA Conf. On Corrosion of Reactor Materials, Salzburg, Austria, STP59, Vol.2, 209-222, 1962.

Averin S. A., et al., "Evolution of dislocation and precipitate structure in Zr alloys under long term irradiation", ASTM STP 1354, pp. 105-121, 2000.

Baily W. E., Marlowe M. O. and Probstle, R. A., "Trends in Nuclear Fuel Performance", Proc. ANS Int'l Topical Meeting LWR Fuel Perform., Orlando, FL, USA, April 21-24, 1985, 1-13-1-15, 1985.

Bentley M. J., "Out-of-Reactor Studies of the Nuclear Oxidation of Zirconium Alloys", U.K. Report, TRG-3001(s), UKAEA, Reactor Fuel Elements Lab, Springfields, Lancs, 1977.

Bergmann C. A., Jacko R., Roesmer J. and Miller R., "PWR Primary System Chemistry: Experience with Elevated pH at Millstone Point Unit 3", Proc. BNES Conf. Water Chem. Nucl. Reactor Syst. 5 Bournemouth 23-27 Oct. 1989, Vol. 2, Paper 4, 7–12, 1989.

Bernard L.C., Rebeyrolle V., Van Schel E., Foissaud C. and Wesley D.A., "The Framatome Copernic Fuel Rod Performance Code,Recent High Burnup and Advanced Cladding Developments", Proc: ANS Light Water Reactor Fuel Performance, Park City, Utah, USA, 2000.

Besch O. A., et al., "Corrosion behavior of DUPLEX and referece cladding in NNP Grohnde", ASTM STP 1295, pp. 805-824, 1996.

Billot Ph., et al., "Developments of a mechanistic model to assess the external corrosion of the Zircaloy cladding in PWRs", Zirconium in the Nuclear Industry: 8th Int. SytnpASTM-STP-1023, Eds.Van Swam, L. F. P., Eucken, C. M., American Society for Testing and Materials, W. Conshohocken, Pä. 165-184, 1989.

Billot, P., Beslu, P., Giordano, A. and Thomazet, J.,
"Development of a Mechanistic Model to Assess the External Corrosion of the Zircaloy Claddings in PWR's", Proc. 8th Int. Symp. on Zr in the Nucl. Ind., San Diego, USA, 1988, ASTM-STP-1023, pp165-184.

Billot Ph. and Giordano A., "Comparison of Zircaloy corrosion models from the evaluation of in-reactor and out-of-pile loop performance", ASTM-STP 1132, pp.539-567, 1991.

Billot P., Beslu P., Robin J. C., "Consequences of lithium incorporation in oxide films due to irradiation effect", Fuel for the 90's, (Int. Topical Mtg. On LWR Fuel Performance), Avignon, France, Vol. 2, American Nuclear Soc./European Nuclear Soc., 757-769, 1991.

Billot Ph., et al., "Experimental and theoretical studies of parameters that influence corrosion of Zircasloy-4", ASTM STP 1245, pp. 351-377, 1994.

Billot, P., Robin, J.C., Giordano, A., Peybernès, Thomazet, J., and Amanrich, H.,
"Experimental and Theoretical Studies of Parameters that Influence Corrosion of Zircaloy-4",
Proc. 10th Int. Symp. on Zr in the Nucl. Ind., Baltimore, USA, 1993, ASTM-STP-1245, pp351-377.

Billot P., Robin J-C., Giordano A., Peybernes J., Thomazet J. and Amanrich, H., "Experimental and theoretical studies of parameters that Influence corrosion of Zircaloy-4", Zirconium in the Nuclear Industry: 10th Int. Symp., ASTM-STP1245, Eds., Garde, A. M., Bradley, E. R., American Society for Testing and Materials, W. Conshohocken, pp. 351-375, 1994.

Billot Ph., et al., "Corrosion of Zircasloy-4 under demanding PWR-type conditions", presented at the 13th ASTM-Zr Conference in Annecy in June 2001.

Blat, M. and Bourgoin, J., "Corrosion Behavior of Zircaloy Cladding Material: Evaluation of the Hydriding Effect", International Topical Meeting on Light Water Reactor Fuel Performance, ANS, Portland , Oregon, pp. 250-257, 1997

Blat M., Legras L., Noel D. and Amanrich H., "Contribution to a Better Understanding of the Detrimental Role of Hydrogen on the Corrosion Rate of Zry-4 Cladding Materials, Zirconium in the Nuclear Industry: 12th Int'l Symposium, ASTM STP 1354, G. Sabol and G. Moan, Eds. ASTM, West Conshohocken, PA, 563-591, 2000.

Bradhurst D. H., Draley J. E. and Van Drunen C. J., J. Electrochem. Soc., 112, 1171-1177, 1965.

Bramwell I. L., Parsons P. D. and Tice D. R., "Corrosion of Zircaloy-4 PWR Fuel Cladding in Lithiated and Borated Water Environments" Proc. 9th Int. Symp. On Zr in the Nuclear Ind., Kobe Jp., ASTM – STP – 1132, 628-642, 1991.

Brossman U., Würschurm R., Södervall U. and Schafer H. E., J. Appl. Phys., 85 7646-7654, 1999.

Broy Y., Garzarolli F., Seibold A. and Van Swam L. F., "Influence of Transition Elements Fe, Cr, and V on Long-Time Corrosion in PWRs", Zirconium in the Nuclear Industry: 12th Int'l Symposium, ASTM STP 1354, G. P. Sabol and G. D. Moan, Eds., ASTM, West Conshohocken, PA, 609-622, 2000.

Bryant P. E. C., "Round-Robin Tests to Develop a Standard Autoclave Testing Procedure for Zirconium Alloys", Applications-Related Phenomena for Zirconium and Its Alloys, ASTM STP 458, ASTM, 360-371, 1969.

Bryner J. A., J. Nuclear Mater., 82, 84-101, 1979.

Cabrera N. and Mott N. F., Reps. Prog. Phys, 12, 163, 1949.

CANDU Pressure Tubes, Proc. 5th Int. Conf. On Microscopy of Oxidation, Limerick, Eire,. to be published.

Charquet D. and Alheritiere E., "Influence of Impurities and Temperature on the microstructure of ircaloy-4 and Zircaloy-2 after the beta-alpha phase transformation", ASTM STP 939, pp. 284-291, 1987.

Charquet D., Steinberg E. and Millet Y., "Influence of Variations in Early Fabrications Steps on Corrosion, Mechanical Properties, and Structure of Zircaloy-4 Products", Zirconium in the Nuclear Industry: 7th Int'l Symposium, ASTM STP 939, Adamson R. B. and Van Swam L. F. P., Eds., ASTM, Philadelphia, 431-447, 1987.

Charquet D., et al., "Solubility limits and Formation of intermetallic precipitates in ZrSnFeCr alloys", ASTM STP 1023, pp. 405-422, 1988.